Journal of Elasticity **59:** 23–50, 2000.

Derivation of Plate and Rod Equations for a Piezoelectric Body from a Mixed Three-Dimensional Variational Principle

S. VIDOLI[1] and R.C. BATRA[2]
[1]*Dipartimento di Ingegneria Strutturale e Geotecnica, Universitá di Roma "La Sapienza", 00184 Roma, Italy*
[2]*Department of Engineering Science and Mechanics, MC 0219, Virginia Polytechnic Institute and State University, Blacksburg, VA 24061, U.S.A.*

Received 16 December 1998; in revised form 24 January 2000

Dedicated to Roger Fosdick on the occasion of his 60th birthday.

Abstract. We use a mixed 3-dimensional variational principle to derive 2-dimensional equations for an anisotropic plate-like piezoelectric body and one-dimensional equations for an anisotropic beam-like piezoelectric body. The formulation accounts for double forces without moments which may change the thickness of the plate and deform the cross-section of the rod. The dependence of the bending rigidities of a transversely isotropic plate upon the angle between the normal to the midsurface and the direction of transverse isotropy is exhibited. The plate equations are used to study the cylindrical deformations of a transversely isotropic plate due to equal and opposite charges applied to its top and bottom surfaces. It is also found that a piezoelectric circular rod with axis of transverse isotropy not coincident with its centroidal axis and subjected to electric charges at the end faces is deformed into a non-prismatic body.

Mathematics Subject Classifications (1991): 74E10, 74E30.

Key words: electroelasticity, approximate theories, anisotropic bodies, double forces.

1. Introduction

Mindlin [1] derived a 2-dimensional theory for plates by expanding displacements as power series in the transverse direction, and integrating the 3-dimensional balance laws and linear constitutive relations in the thickness direction. He proposed correction factors in order for the response predicted from the 2-dimensional theory to match with that deduced from the 3-dimensional linear elasticity theory. He [2] generalized these to piezoelectric plates by also expanding the electric potential as a power series in the transverse direction. Reissner [3] derived a plate theory from the 3-dimensional elasticity theory by using a mixed variational principle, now known as the Hellinger–Prange–Reissner principle. This principle admits different

hypotheses on the stress and displacement fields, and has also been employed by Ciarlet and Destuynder [4] to derive the Kirchhoff–Love plate theory. These and other attempts to systematically derive plate and rod theories have been reviewed by Koiter and Simmonds [5], Naghdi [6], Antman [7] and Leissa [8] among others. Naghdi [6] and Antman [7] have also discussed the Cosserat [9] direct theories of plates and rods wherein the bodies are modeled as 2-dimensional surfaces or one-dimensional curves with a suitable number of directors attached to each point; these directors are not tangent to the surface or the curve. The deformation of the directors accounts for the transverse deformations of the plate and of the area of cross-section of the rod. Ericksen [10] has studied plane waves in plates by using such a theory. Because of the immense literature on plates and rods, it is nearly impossible to cite all of the significant contributions.

Podio-Guidugli [11] has used the method of internal constraints to deduce equations of thin plates from the 3-dimensional elasticity equations. He accounted for the material symmetry and the indeterminacy in the stresses induced by the kinematic constraints. Nicotra and Podio-Guidugli [12] have employed the principle of virtual work to derive equations for a plate-like transversely isotropic piezoelectric body by assuming that the displacements and the electric potential vary affinely in the transverse direction. They assumed that the axis of transverse isotropy coincides with the normal to the midsurface of the plate. Their plate equations exhibit uncoupling between the membrane and bending effects. Teresi and Tiero [13] deduced plate theories by seeking stationary points in suitable subspaces of the functional spaces in which the potential energy, the complementary energy and the Hellinger–Prange–Reissner functionals are defined. For an isotropic plate they showed that these methods give different values of the flexural and shear rigidities.

Yang and Batra [14] have given variational principles for piezoelectric bodies. Here we use one of their mixed variational principles (i.e., a generalization of the Hellinger–Prange–Reissner principle to piezoelectric bodies) to derive equilibrium equations and constitutive relations for anisotropic plate-like and rod-like piezoelectric bodies. These equations are used to analyze cylindrical deformations of a transversely isotropic plate with equal and opposite charges applied to its top and bottom surfaces. We also investigate the dependence of the deformations of the plate on the angle between the axis of transverse isotropy and the unit normal to the midsurface of the plate. A similar problem is studied for a transversely isotropic rod. The axial elongations of the rod are significantly increased when the deformations of its cross-sections are considered.

2. Formulation of the Problem

We consider a prismatic anisotropic linear piezoelectric body occupying the region $\mathcal{P} = \mathcal{S} \times \mathcal{I}$ where $\mathcal{S} \subset \mathbb{R}^2$ is a plane surface and $\mathcal{I} = (-h, h)$. For a plate, $\mathcal{S}$ can be identified with its midsurface and $2h$ equals the thickness of the plate. For a prismatic bar, $\mathcal{S}$ is a cross-section and $2h$ the length. The boundary $\partial\mathcal{P}$ of $\mathcal{P}$ can

be written as $(\partial\mathcal{S}\times\mathcal{I})\cup(\mathcal{S}^+\cup\mathcal{S}^-)=\mathcal{M}\cup\mathcal{B}$ where $\partial\mathcal{S}$ is the periphery of $\mathcal{S}$, and $\mathcal{S}^+$ and $\mathcal{S}^-$ the upper and lower surfaces of $\mathcal{P}$, i.e., $\mathcal{S}^+=\mathcal{S}\times\{h\}$, and $\mathcal{S}^-=\mathcal{S}\times\{-h\}$. $\mathcal{M}$ is called the mantle of $\mathcal{P}$ and $\mathcal{B}$ is the union of upper and lower bases.

The mixed variational principle of Yang and Batra [14, equation (29)] for quasistatic deformations of a linear piezoelectric body can be written as follows. Find a saddle point of the functional

$$\begin{aligned}\mathcal{H}(\mathbf{u},\mathbf{S},\psi,\mathbf{D}) \;=\; &\int_{\mathcal{P}}\mathbf{b}\cdot\mathbf{u}+\int_{\partial_a\mathcal{P}}\mathbf{S}\mathbf{n}\cdot\big(\mathbf{u}-\bar{\mathbf{u}}\big)+\int_{\partial_b\mathcal{P}}\mathbf{f}\cdot\mathbf{u}-\int_{\mathcal{P}}\mathbf{S}\cdot\mathbf{E}(\mathbf{u})\\ &+\int_{\mathcal{P}}q\,\psi+\int_{\partial_\alpha\mathcal{P}}\mathbf{D}\cdot\mathbf{n}\big(\psi-\bar{\psi}\big)+\int_{\partial_\beta\mathcal{P}}\chi\,\psi-\int_{\mathcal{P}}\mathbf{D}\cdot\mathbf{W}(\psi)\\ &+\frac{1}{2}\int_{\mathcal{P}}\big[\mathbf{S}\cdot(\mathbb{F}\,\mathbf{S}+\mathbb{M}\mathbf{D})+\mathbf{D}\cdot\big(\mathbb{N}\mathbf{D}-\mathbb{M}^{\mathrm{T}}\mathbf{S}\big)\big],\end{aligned}\tag{1}$$

where $\mathbf{E}(\mathbf{u})=\mathrm{SYM}\,\mathrm{GRAD}\,\mathbf{u}$, $\mathbf{W}(\psi)=\mathrm{GRAD}\,\psi$, and

$$\begin{aligned}&\partial_a\mathcal{P}\cup\partial_b\mathcal{P}=\partial\mathcal{P}, \qquad &&\partial_a\mathcal{P}\cap\partial_b\mathcal{P}=\emptyset,\\ &\partial_\alpha\mathcal{P}\cup\partial_\beta\mathcal{P}=\partial\mathcal{P}, \qquad &&\partial_\alpha\mathcal{P}\cap\partial_\beta\mathcal{P}=\emptyset.\end{aligned}\tag{2}$$

Here $\mathbf{u}$ is the displacement of the body point $\mathbf{x}$, GRAD is the 3-dimensional gradient operator with respect to $\mathbf{x}$, $\mathrm{SYM}\,\mathrm{GRAD}\,\mathbf{u}=(\mathrm{GRAD}\,\mathbf{u}+(\mathrm{GRAD}\,\mathbf{u})^{\mathrm{T}})/2$, $\mathbf{b}$ the density of the body force, $\mathbf{f}$ the surface traction, $\mathbf{S}$ the stress tensor, $\mathbf{n}$ a unit outward normal to $\partial\mathcal{P}$, q the volume charge density, ψ the electric potential, χ the surface charge density, $\mathbf{D}$ the electric displacement, $\mathbf{W}$ the electric field, $\bar{\mathbf{u}}$ the displacements prescribed on $\partial_a\mathcal{P}$, $\bar{\psi}$ the electric potential prescribed on $\partial_\alpha\mathcal{P}$, and

$$\mathbf{E}=\mathbb{F}\mathbf{S}+\mathbb{M}\mathbf{D}, \qquad \mathbf{W}=\mathbb{N}\mathbf{D}-\mathbb{M}^{\mathrm{T}}\mathbf{S},\tag{3}$$

are the constitutive relations for a general anisotropic piezoelectric body. $\mathbb{F}$ is the compliance matrix, $\mathbb{M}$ describes the coupling between the electrical and mechanical effects, and $\mathbb{N}$ is the matrix of dielectric permittivities. We note that electric quantities analogous to mechanical quantities $\mathbf{b}$, $\mathbf{S}$, $\mathbf{f}$, $\mathbf{u}$ and $\mathbf{E}$ are q, $\mathbf{D}$, χ, ψ and $\mathbf{W}$, respectively.

For a prismatic body, a natural decomposition of the position vector, the displacement field and the outward unit normal is

$$\mathbf{x}=\mathbf{r}+\zeta\mathbf{e}, \qquad \mathbf{u}=\mathbf{v}+w\,\mathbf{e}, \qquad \mathbf{n}=\boldsymbol{\nu}+n\mathbf{e},\tag{4}$$

where $\mathbf{e}$ is a unit vector perpendicular to $\mathcal{S}$. Thus $\mathbf{v}$ and w denote the displacements of a point within and perpendicular to $\mathcal{S}$. The other field variables can now be written as

$$
\begin{aligned}
\mathbf{E}(\mathbf{u}) &= \text{SYM GRAD}\mathbf{v} + \frac{\mathbf{v}' + \text{GRAD}w}{2} \otimes \mathbf{e} + \mathbf{e} \otimes \frac{\mathbf{v}' + \text{GRAD}w}{2} + w'\mathbf{e} \otimes \mathbf{e}, \\
&= \widehat{\mathbf{E}} + \boldsymbol{\gamma} \otimes \mathbf{e} + \mathbf{e} \otimes \boldsymbol{\gamma} + \varepsilon \mathbf{e} \otimes \mathbf{e}, \\
\mathbf{W}(\psi) &= \text{GRAD}\psi + \psi'\mathbf{e} = \widehat{\mathbf{W}} + \omega\mathbf{e}, \\
\mathbf{S} &= \widehat{\mathbf{S}} + \mathbf{s} \otimes \mathbf{e} + \mathbf{e} \otimes \mathbf{s} + \sigma \mathbf{e} \otimes \mathbf{e}, \\
\mathbf{D} &= \widehat{\mathbf{D}} + \delta\mathbf{e}, \qquad \mathbf{b} = \hat{\mathbf{b}} + \beta\mathbf{e}, \qquad \mathbf{f} = \hat{\mathbf{f}} + \varphi\mathbf{e},
\end{aligned}
\tag{5}
$$

and the constitutive relations (3) become

$$
\begin{Bmatrix} \widehat{\mathbf{E}} \\ \boldsymbol{\gamma} \\ \varepsilon \\ \widehat{\mathbf{W}} \\ \omega \end{Bmatrix} =
\begin{bmatrix}
\mathbb{F}_{ES} & \mathbb{F}_{Es} & \mathbb{F}_{E\sigma} & \mathbb{M}_{ED} & \mathbb{M}_{E\delta} \\
* & \mathbb{F}_{\gamma s} & \mathbb{F}_{\gamma\sigma} & \mathbb{M}_{\gamma D} & \mathbb{M}_{\gamma\delta} \\
* & * & \mathbb{F}_{\varepsilon\sigma} & \mathbb{M}_{\varepsilon D} & \mathbb{M}_{\varepsilon\delta} \\
-* & -* & -* & \mathbb{N}_{WD} & \mathbb{N}_{W\delta} \\
-* & -* & -* & * & \mathbb{N}_{\omega\delta}
\end{bmatrix}
\begin{Bmatrix} \widehat{\mathbf{S}} \\ \mathbf{s} \\ \sigma \\ \widehat{\mathbf{D}} \\ \delta \end{Bmatrix},
\tag{6}
$$

where $w' = \partial w/\partial\zeta$, a $*$ in row i and column j represents the transpose of the entry in row j and column i, and the tensor product $\otimes$ between two vectors $\mathbf{a}$ and $\mathbf{b}$ is defined by $(\mathbf{a} \otimes \mathbf{b})\mathbf{c} = (\mathbf{b} \cdot \mathbf{c})\mathbf{a}$ for an arbitrary vector $\mathbf{c}$. In terms of fields (5), equation (1) becomes

$$
\begin{aligned}
&\mathcal{H}\big(\mathbf{v}, w, \widehat{\mathbf{S}}, \mathbf{s}, \sigma, \psi, \widehat{\mathbf{D}}, \delta\big) \\
&\quad = \int_{\mathcal{P}} (\hat{\mathbf{b}} \cdot \mathbf{v} + \beta w) \\
&\qquad + \int_{\partial_a\mathcal{P}} \big[(\widehat{\mathbf{S}}\boldsymbol{\nu} + \mathbf{s}n) \cdot (\mathbf{v} - \bar{\mathbf{v}}) + (\mathbf{s} \cdot \boldsymbol{\nu} + \sigma n)(w - \bar{w})\big] \\
&\qquad + \int_{\partial_b\mathcal{P}} \big(\hat{\mathbf{f}} \cdot \mathbf{v} + \varphi w\big) - \int_{\mathcal{P}} \big(\widehat{\mathbf{S}} \cdot \widehat{\mathbf{E}} + 2\mathbf{s} \cdot \boldsymbol{\gamma} + \sigma\varepsilon\big) \\
&\qquad + \int_{\mathcal{P}} q\psi + \int_{\partial_\alpha\mathcal{P}} \big[\big(\widehat{\mathbf{D}} \cdot \boldsymbol{\nu} + \delta n\big)(\psi - \bar{\psi})\big] \\
&\qquad + \int_{\partial_\beta\mathcal{P}} \chi\psi - \int_{\mathcal{P}} \big(\widehat{\mathbf{D}} \cdot \widehat{\mathbf{W}} + \delta\omega\big) \\
&\qquad + \frac{1}{2}\Bigg[\int_{\mathcal{P}} \widehat{\mathbf{S}} \cdot \big(\mathbb{F}_{ES}\widehat{\mathbf{S}} + \mathbb{F}_{Es}\mathbf{s} + \mathbb{F}_{E\sigma}\sigma + \mathbb{M}_{ED}\widehat{\mathbf{D}} + \mathbb{M}_{E\delta}\delta\big) \\
&\qquad + \int_{\mathcal{P}} \mathbf{s} \cdot \big(\mathbb{F}_{Es}^{\mathrm{T}}\widehat{\mathbf{S}} + \mathbb{F}_{\gamma s}\mathbf{s} + \mathbb{F}_{\gamma\sigma}\sigma + \mathbb{M}_{\gamma D}\widehat{\mathbf{D}} + \mathbb{M}_{\gamma\delta}\delta\big) \\
&\qquad + \int_{\mathcal{P}} \sigma\big(\mathbb{F}_{E\sigma}^{\mathrm{T}}\widehat{\mathbf{S}} + \mathbb{F}_{\gamma\sigma}^{\mathrm{T}}\mathbf{s} + \mathbb{F}_{\varepsilon\sigma}\sigma + \mathbb{M}_{\varepsilon D}\widehat{\mathbf{D}} + \mathbb{M}_{\varepsilon\delta}\delta\big) \\
&\qquad + \int_{\mathcal{P}} \widehat{\mathbf{D}} \cdot \big(\mathbb{N}_{WD}\widehat{\mathbf{D}} + \mathbb{N}_{W\delta}\delta - \mathbb{M}_{ED}^{\mathrm{T}}\widehat{\mathbf{S}} - \mathbb{M}_{\gamma D}^{\mathrm{T}}\mathbf{s} - \mathbb{M}_{\varepsilon D}^{\mathrm{T}}\sigma\big) \\
&\qquad + \int_{\mathcal{P}} \delta\big(\mathbb{N}_{W\delta}^{\mathrm{T}}\widehat{\mathbf{D}} + \mathbb{N}_{\omega\delta}\delta - \mathbb{M}_{E\delta}^{\mathrm{T}}\widehat{\mathbf{S}} - \mathbb{M}_{\gamma\delta}^{\mathrm{T}}\mathbf{s} - \mathbb{M}_{\varepsilon\delta}^{\mathrm{T}}\sigma\big)\Bigg],
\end{aligned}
\tag{7}
$$

where $\mathbf{A} \cdot \mathbf{B} = \text{tr}\,(\mathbf{A}\mathbf{B}^{\mathrm{T}})$ for tensors $\mathbf{A}$ and $\mathbf{B}$.

3. Plate-like Bodies

For a plate-like body, displacements and electric potentials are not prescribed on $\mathcal{S}^+$ and $\mathcal{S}^-$. However, displacements and/or surface tractions, and electric potentials and/or charges may be prescribed on the mantle of the body. Thus,

$$\begin{aligned} &\partial_a\mathcal{P} = \mathcal{M}_a, \qquad &&\partial_\alpha\mathcal{P} = \mathcal{M}_\alpha, \\ &\partial_b\mathcal{P} = \mathcal{M}_b \cup \mathcal{B}, \quad &&\partial_\beta\mathcal{P} = \mathcal{M}_\beta \cup \mathcal{B}. \end{aligned} \tag{8}$$

The displacement fields $\mathbf{v}$ and w and electric potential ψ are taken to be affine functions of ζ. That is,

$$\begin{aligned} &\mathbf{v}(\mathbf{r},\zeta) = \mathbf{v}_0(\mathbf{r}) + \zeta\mathbf{v}_1(\mathbf{r}), \qquad &&w(\mathbf{r},\zeta) = w_0(\mathbf{r}) + \zeta w_1(\mathbf{r}), \\ &\psi(\mathbf{r},\zeta) = \psi_0(\mathbf{r}) + \zeta\psi_1(\mathbf{r}). \end{aligned} \tag{9}$$

The representation $(9)_2$ for the transverse displacement allows for a change in the thickness of the plate. Vel and Batra [15] have used the 3-dimensional equations of elastostatics to analyze deformations of a linear elastic orthotropic plate. They found that the elongation of the normal to the midsurface of the plate is in general nonzero and depends upon the boundary conditions at the plate edges and the loading. Representations (9) for $\mathbf{u}$ and ψ are the same as those assumed by Nicotra and Podio-Guidugli [12], and the representation $(9)_2$ for w is more general than that of Teresi and Tiero [13]. For displacements and the electric potential given by (9), we have

$$\begin{aligned} &\widehat{\mathbf{E}} = \text{SYM GRAD}\mathbf{v}_0 + \zeta\,\text{SYM GRAD}\mathbf{v}_1 =: \widehat{\mathbf{E}}_0 + \zeta\widehat{\mathbf{E}}_1, \\ &2\boldsymbol{\gamma} = \mathbf{v}_1 + \text{GRAD}\, w_0 + \zeta\,\text{GRAD}w_1 =: \boldsymbol{\gamma}_0 + \zeta\boldsymbol{\gamma}_1, \\ &\varepsilon = w_1 =: \varepsilon_0, \qquad \widehat{\mathbf{W}} = \text{GRAD}\psi_0 + \zeta\,\text{GRAD}\psi_1 =: \widehat{\mathbf{W}}_0 + \zeta\widehat{\mathbf{W}}_1, \\ &\omega = \psi_1 =: \omega_0. \end{aligned} \tag{10}$$

$\widehat{\mathbf{E}}_0$ is called the membranal strain tensor, $\widehat{\mathbf{E}}_1$ the curvature tensor, and $\boldsymbol{\gamma}$ the shear strain vector. Note that $\boldsymbol{\gamma}$ varies affinely through the thickness. The functional $\mathcal{H}$ given in (7) now becomes

$$\begin{aligned} \mathcal{H} = &\int_{\mathcal{S}} (\mathbf{B}_0\cdot\mathbf{v}_0 + \mathbf{B}_1\cdot\mathbf{v}_1 + \Xi_0 w_0 + \Xi_1 w_1 + Q_0\psi_0 + Q_1\psi_1) \\ &+ \int_{\partial_b\mathcal{S}} (\mathbf{F}_0\cdot\mathbf{v}_0 + \mathbf{F}_1\cdot\mathbf{v}_1 + \Phi_0 w_0 + \Phi_1 w_1) + \int_{\partial_\beta\mathcal{S}} (X_0\psi_0 + X_1\psi_1) \\ &+ \int_{\mathcal{S}} (\text{DIV}\mathbf{N})\cdot\mathbf{v}_0 + (\text{DIV}\mathbf{M} + \mathbf{T})\cdot\mathbf{v}_1 + (\text{DIV}\mathbf{T})w_0 \\ &+ (\text{DIV}\mathbf{C} + \Sigma)w_1 + (\text{DIV}\boldsymbol{\Delta}_0)\psi_0 + (\text{DIV}\boldsymbol{\Delta}_1 + d)\psi_1] \\ &- \int_{\partial_b\mathcal{S}} \big[(\mathbf{N}\boldsymbol{\nu})\cdot\mathbf{v}_0 + (\mathbf{M}\boldsymbol{\nu})\cdot\mathbf{v}_1 + (\mathbf{T}\cdot\boldsymbol{\nu})w_0 + (\mathbf{C}\cdot\boldsymbol{\nu})w_1\big] \\ &- \int_{\partial_\beta\mathcal{S}} \big[(\boldsymbol{\Delta}_0\cdot\boldsymbol{\nu})\psi_0 + (\boldsymbol{\Delta}_1\cdot\boldsymbol{\nu})\psi_1\big] + \mathcal{R}\big(\widehat{\mathbf{S}}, \mathbf{s}, \sigma, \widehat{\mathbf{D}}, \delta\big), \end{aligned} \tag{11}$$

where

$$
\begin{aligned}
&\mathbf{B}_0 = \big(\hat{\mathbf{f}}^+ - \hat{\mathbf{f}}^-\big) + \int_{\mathcal{I}} \hat{\mathbf{b}}, \qquad \mathbf{B}_1 = h\big(\hat{\mathbf{f}}^+ + \hat{\mathbf{f}}^-\big) + \int_{\mathcal{I}} \zeta \hat{\mathbf{b}},\\
&\mathbf{F}_0 = \int_{\mathcal{I}} \hat{\mathbf{f}}, \qquad\qquad\qquad \mathbf{F}_1 = \int_{\mathcal{I}} \zeta \hat{\mathbf{f}},\\
&\Xi_0 = \big(\varphi^+ - \varphi^-\big) + \int_{\mathcal{I}} \beta, \qquad \Xi_1 = h\big(\varphi^+ + \varphi^-\big) + \int_{\mathcal{I}} \zeta\beta,\\
&\Phi_0 = \int_{\mathcal{I}} \varphi, \qquad\qquad\qquad \Phi_1 = \int_{\mathcal{I}} \zeta\varphi,\\
&Q_0 = (\chi^+ - \chi^-) + \int_{\mathcal{I}} q, \qquad Q_1 = h(\chi^+ + \chi^-) + \int_{\mathcal{I}} \zeta q,\\
&X_0 = \int_{\mathcal{I}} \chi, \qquad X_1 = \int_{\mathcal{I}} \zeta\chi,\\
&\mathbf{N} = \int_{\mathcal{I}} \widehat{\mathbf{S}}, \qquad \mathbf{M} = \int_{\mathcal{I}} \zeta\widehat{\mathbf{S}}, \qquad \mathbf{T} = \int_{\mathcal{I}} \mathbf{s}, \qquad \mathbf{C} = \int_{\mathcal{I}} \zeta\mathbf{s},\\
&\Sigma = \int_{\mathcal{I}} \sigma, \qquad \boldsymbol{\Delta}_0 = \int_{\mathcal{I}} \widehat{\mathbf{D}}, \qquad \boldsymbol{\Delta}_1 = \int_{\mathcal{I}} \zeta\widehat{\mathbf{D}}, \qquad d = \int_{\mathcal{I}} \delta,\\
&\hat{\mathbf{f}}^\pm = \mathbf{s}n^\pm, \quad \varphi^\pm = \sigma n^\pm, \qquad \chi^\pm = \delta n^\pm, \quad \text{on } \mathcal{S}^\pm,
\end{aligned}
\tag{12}
$$

and $\mathcal{R}(\widehat{\mathbf{S}}, \mathbf{s}, \sigma, \widehat{\mathbf{D}}, \delta)$ is the part of $\mathcal{H}$ that does not depend upon the displacements and the electric potential. Superscripts $+$ and $-$ on a quantity signify its values on surfaces $\mathcal{S}^+$ and $\mathcal{S}^-$ respectively. Here $\mathbf{N}$ is a 2×2 symmetric matrix giving the in-plane (within the plane $\mathcal{S}$) forces sometimes also called the membranal stress tensor, DIV is the 2-dimensional (within the plane $\mathcal{S}$) divergence operator, $\mathbf{M}$ is the 2×2 symmetric matrix of bending moments also called the moment tensor, $\mathbf{T}$ is the resultant shear force or the shear stress vector, $\mathbf{C}$ is the moment of internal double forces (i.e., of forces acting along $\mathbf{e}$), Σ is the resultant transverse normal stress, $\boldsymbol{\Delta}_0$ is the resultant in-plane electric displacement, $\boldsymbol{\Delta}_1$ represents the resultant moment of order 1 of the in-plane electric displacement, and d is the resultant transverse electric displacement. $\mathbf{B}_0 + \Xi_0\mathbf{e}$ is the resultant body force per unit area of $\mathcal{S}$, $\mathbf{B}_1$ the body couple per unit area, Q_0 the resultant applied charge/area, Q_1 the resultant moment of the electric charge, Ξ_1 the double force per unit area, and $\mathbf{F}_0$, $\mathbf{F}_1$, Φ_0, Φ_1 and X_0 have meanings similar to those of $\mathbf{B}_0$, $\mathbf{B}_1$, Ξ_0, Ξ_1 and Q_0 but are defined on the boundary $\partial\mathcal{S}$ of $\mathcal{S}$. The variation of $\mathcal{H}$ with respect to $\mathbf{v}_0$, $\mathbf{v}_1$, w_0, w_1, ψ_0 and ψ_1 gives

$$
\begin{aligned}
&\text{DIV}\mathbf{N} + \mathbf{B}_0 = \mathbf{0}, \quad \text{DIV}\mathbf{M} + \mathbf{T} + \mathbf{B}_1 = \mathbf{0}, \quad \text{DIV}\mathbf{T} + \Xi_0 = 0, \quad \text{on } \mathcal{S},\\
&\text{DIV}\mathbf{C} + \Sigma + \Xi_1 = 0, \quad \text{DIV}\boldsymbol{\Delta}_0 + Q_0 = 0, \quad \text{DIV}\boldsymbol{\Delta}_1 + d + Q_1 = 0, \ \text{on } \mathcal{S},\\
&\mathbf{N}\nu = \mathbf{F}_0, \quad \mathbf{M}\nu = \mathbf{F}_1, \quad \mathbf{T}\cdot\boldsymbol{\nu} = \Phi_0, \quad \mathbf{C}\cdot\boldsymbol{\nu} = \Phi_1, \quad \text{on } \partial_b\mathcal{S},\\
&\boldsymbol{\Delta}_0\cdot\boldsymbol{\nu} = X_0, \quad \boldsymbol{\Delta}_1\cdot\boldsymbol{\nu} = X_1, \quad \text{on } \partial_\beta\mathcal{S}.
\end{aligned}
\tag{13}
$$

We assume that the stress fields $\widehat{\mathbf{S}}$, $\mathbf{s}$ and σ, and the electric displacements $\widehat{\mathbf{D}}$ and δ are polynomials in ζ of degree 1, 3, 2, 1 and 2, respectively. This is guided by the forms of equations $(12)_{11}$–$(12)_{17}$, and the boundary conditions on $\mathbf{s}$, σ and δ at the top and bottom surfaces $\mathcal{S}^+$ and $\mathcal{S}^-$. Recall that tractions and electric charges applied on $\mathcal{S}^+$ and $\mathcal{S}^-$ are included in $(12)_1$, $(12)_2$, $(12)_5$, $(12)_6$ and $(12)_9$. The assumption that $\widehat{\mathbf{S}}$, $\mathbf{s}$, σ, $\widehat{\mathbf{D}}$ and δ are polynomials in ζ of degrees higher than 1, 3, 2, 1 and 2 respectively leads to an indeterminate set of equations. Of course, one could postulate criteria for the determination of the higher-order terms and endow more structure to the 2-dimensional model. Our choice uses the lowest degree polynomials for satisfying $(12)_{11}$–$(12)_{17}$ and the boundary conditions on $\mathcal{S}^+$ and $\mathcal{S}^-$. Thus, we take

$$
\begin{aligned}
\widehat{\mathbf{S}}(\mathbf{r},\zeta) &= \frac{\mathbf{N}(\mathbf{r})}{2h} + \zeta\frac{\mathbf{M}(\mathbf{r})}{J},\\
\mathbf{s}(\mathbf{r},\zeta) &= \frac{3}{4h}\left(1-\frac{\zeta^2}{h^2}\right)\mathbf{T}(\mathbf{r}) + \frac{5}{2J}\left(\zeta-\frac{\zeta^3}{h^2}\right)\mathbf{C}(\mathbf{r})\\
&\quad -\frac{1}{2}\left[\hat{\mathbf{f}}_1\left(1-\frac{3\zeta^2}{h^2}\right)+\hat{\mathbf{f}}_0\frac{\zeta}{h}\left(3-5\frac{\zeta^2}{h^2}\right)\right],\\
\sigma(\mathbf{r},\zeta) &= \frac{3}{4h}\left(1-\frac{\zeta^2}{h^2}\right)\Sigma(\mathbf{r}) - \frac{1}{2}\left[\varphi_1\left(1-\frac{3\zeta^2}{h^2}\right)-2\varphi_0\frac{\zeta}{h}\right],\\
\widehat{\mathbf{D}}(\mathbf{r},\zeta) &= \frac{\boldsymbol{\Delta}_0(r)}{2h} + \frac{\zeta\,\boldsymbol{\Delta}_1(\mathbf{r})}{J},\\
\delta(\mathbf{r},\zeta) &= \frac{3}{4h}\left(1-\frac{\zeta^2}{h^2}\right)d - \frac{1}{2}\left[\chi_1\left(1-\frac{3\zeta^2}{h^2}\right)-2\chi_0\frac{\zeta}{h}\right],
\end{aligned}
\tag{14}
$$

where $J = \int_{\mathcal{I}}\zeta^2 = (2h^3)/3$,

$$
\begin{aligned}
\hat{\mathbf{f}}_1 &= \frac{1}{2}\big(\hat{\mathbf{f}}^+ + \hat{\mathbf{f}}^-\big), \qquad & \hat{\mathbf{f}}_0 &= \frac{1}{2}\big(\hat{\mathbf{f}}^+ - \hat{\mathbf{f}}^-\big),\\
\varphi_1 &= \frac{1}{2}\big(\varphi^+ + \varphi^-\big), \qquad & \varphi_0 &= \frac{1}{2}\big(\varphi^+ - \varphi^-\big),\\
\chi_1 &= \frac{1}{2}\big(\chi^+ + \chi^-\big), \qquad & \chi_0 &= \frac{1}{2}\big(\chi^+ - \chi^-\big).
\end{aligned}
\tag{15}
$$

The variation of $\mathcal{H}$ with respect to $\mathbf{N}$, $\mathbf{M}$, $\mathbf{T}$, $\mathbf{C}$, Σ, $\boldsymbol{\Delta}$ and d gives

$$
\begin{Bmatrix} \widehat{\mathbf{E}}_0 \\ \boldsymbol{\gamma}_0 \\ \varepsilon_0 \\ \widehat{\mathbf{W}}_0 \\ \omega_0 \end{Bmatrix}
= \frac{1}{2h}
\begin{bmatrix}
\mathbb{F}_{ES} & \mathbb{F}_{Es} & \mathbb{F}_{E\sigma} & \mathbb{M}_{ED} & \mathbb{M}_{E\delta}\\
* & \frac{6}{5}\mathbb{F}_{\gamma s} & \frac{6}{5}\mathbb{F}_{\gamma\sigma} & \mathbb{M}_{\gamma D} & \frac{6}{5}\mathbb{M}_{\gamma\delta}\\
* & * & \frac{6}{5}\mathbb{F}_{\varepsilon\sigma} & \mathbb{M}_{\varepsilon D} & \frac{6}{5}\mathbb{M}_{\epsilon\delta}\\
* & * & * & \mathbb{N}_{WD} & \mathbb{N}_{W\delta}\\
-* & -* & -* & * & \frac{6}{5}\mathbb{N}_{\omega\delta}
\end{bmatrix}
\begin{Bmatrix} \mathbf{N} \\ \mathbf{T} \\ \Sigma \\ \boldsymbol{\Delta} \\ d \end{Bmatrix}
$$

$$
\begin{aligned}
&-\frac{1}{5}\begin{Bmatrix} \mathbf{0} \\ \mathbb{F}_{\gamma s}\hat{\mathbf{f}}_1 + \mathbb{F}_{\gamma\sigma}\varphi_1 + \mathbb{M}_{\gamma\delta}\chi_1 \\ \mathbb{F}^{\mathrm{T}}_{\gamma\sigma}\hat{\mathbf{f}}_1 + \mathbb{F}_{\varepsilon\sigma}\varphi_1 + \mathbb{M}_{\varepsilon\delta}\chi_1 \\ \mathbf{0} \\ \mathbb{M}^{\mathrm{T}}_{\gamma\delta}\hat{\mathbf{f}}_1 + \mathbb{M}_{\varepsilon\delta}\varphi_1 + \mathbb{N}_{\omega\delta}\chi_1 \end{Bmatrix}, \\
\begin{Bmatrix} \hat{\mathbf{E}}_1 \\ \boldsymbol{\gamma}_1 \\ \widehat{\mathbf{W}}_1 \end{Bmatrix} &= \frac{1}{J_S}\begin{bmatrix} \mathbb{F}_{ES} & \mathbb{F}_{Es} & \mathbb{M}_{ED} \\ * & \dfrac{10}{7}\mathbb{F}_{\gamma s} & \mathbb{M}_{\gamma D} \\ -* & -* & \mathbb{N}_{WD} \end{bmatrix}\begin{Bmatrix} \mathbf{M} \\ \mathbf{C} \\ \boldsymbol{\Delta}_1 \end{Bmatrix} \\
&+\begin{Bmatrix} \mathbf{0} \\ -\dfrac{3}{7h}(\mathbb{F}_{\gamma s}\hat{\mathbf{f}}_0 + \mathbb{F}_{\gamma\sigma}\varphi_0 + \mathbb{M}_{\gamma\delta}\chi_0) \\ \mathbf{0} \end{Bmatrix},
\end{aligned}
\tag{16}
$$

$$
\begin{aligned}
&\mathbf{v}_0 = \bar{\mathbf{v}}_0, \quad \mathbf{v}_1 = \bar{\mathbf{v}}_1, \quad w_0 = \overline{w}_0, \quad w_1 = \overline{w}_1, \quad \text{on } \partial_a\mathcal{S}, \\
&\psi_0 = \bar{\psi}_0, \quad \psi_1 = \bar{\psi}_1, \quad \text{on } \partial_\alpha\mathcal{S},
\end{aligned}
\tag{17}
$$

where

$$
\begin{aligned}
&\bar{\mathbf{v}}_0 = \frac{1}{2h}\int_{\mathcal{I}}\bar{\mathbf{v}}, \quad \bar{\mathbf{v}}_1 = \frac{1}{J}\int_{\mathcal{I}}\zeta\bar{\mathbf{v}}, \quad \overline{w}_0 = \frac{3}{4h}\int_{\mathcal{I}}\left(1-\frac{\zeta^2}{h^2}\right)\overline{w}, \\
&\overline{w}_1 = \frac{5}{2J}\int_{\mathcal{I}}\left(\zeta-\frac{\zeta^3}{h^2}\right)\overline{w}, \quad \bar{\psi}_0 = \frac{1}{2h}\int_{\mathcal{I}}\bar{\psi}, \quad \bar{\psi}_1 = \frac{1}{J}\int_{\mathcal{I}}\zeta\bar{\psi}.
\end{aligned}
\tag{18}
$$

Balance laws $(13)_1$–$(13)_6$, constitutive relations (16), boundary conditions $(13)_7$–$(13)_{12}$ and (17), and congruence relations (10) form a complete set of equations for a plate problem. Note that for an anisotropic piezoelectric plate-like body, the problems for the determination of in-plane deformations, shear deformations, changes in thickness that are uniform over $\mathcal{S}$ and the in-plane electric field are coupled together through the constitutive relations. The bending problem is coupled with the problem of determining the thickness variation that is not uniform over $\mathcal{S}$.

Due to the presence of $\mathbf{T}$ in the balance equation $(13)_2$ for $\mathbf{M}$, the transverse shear induces bending of the plate. Also all of the fields are coupled together. A charge applied to $\mathcal{S}^+$ and $\mathcal{S}^-$ will induce bending, shearing, in-plane deformations and variations in the thickness of the plate.

4. Rod-like Bodies

In order to simplify equations, we assume that the ζ-axis coincides with the centroidal axis of the rod. Thus,

$$
\int_{\mathcal{S}}\mathbf{r} = \mathbf{0}. \tag{19}
$$

Furthermore, displacements and electric potentials are assumed to be prescribed only on a part of the upper and lower end faces; however, surface tractions may be prescribed anywhere on the boundary. Thus,

$$\begin{aligned} &\partial_a\mathcal{P} = \mathcal{B}_a, && \partial_\alpha\mathcal{P} = \mathcal{B}_\alpha, \\ &\partial_b\mathcal{P} = \mathcal{M} \cup \mathcal{B}_b, && \partial_\beta\mathcal{P} = \mathcal{M} \cup \mathcal{B}_\beta. \end{aligned} \tag{20}$$

For a rod-like body we assume that $\mathbf{v}$ and w are affine in $\mathbf{r}$, and ψ is uniform over the cross-section. That is

$$\begin{aligned} &\mathbf{v}(\mathbf{r},\zeta) = \mathbf{v}_0(\zeta) + \mathbf{V}(\zeta)\mathbf{r}, \qquad w(\mathbf{r},\zeta) = w_0(\zeta) + \boldsymbol{\varpi}(\zeta)\cdot\mathbf{r}, \\ &\psi(\mathbf{r},\zeta) = \psi_0(\zeta), \end{aligned} \tag{21}$$

where $\mathbf{V}$ is a 2×2 matrix. Thus plane sections remain plane during the deformation process. However, the section is in general not rigid, and can undergo in-plane deformations. The assumption $(21)_3$ for the electric potential is motivated by the common applications of piezoelectric rods where charges are not specified on the rod's mantle. Thus the electric potential can be taken to be uniform over a cross-section. For the displacement and electric potential fields given by (21), we have

$$\begin{aligned} \widehat{\mathbf{E}} &= \mathrm{SYM}\mathbf{V} =: \widehat{\mathbf{E}}_0, \\ 2\boldsymbol{\gamma} &= \mathbf{v}_0' + \boldsymbol{\varpi} + \mathbf{V}'\mathbf{r} =: \boldsymbol{\gamma}_0 + \boldsymbol{\Gamma}\mathbf{r}, \\ \varepsilon &= w_0' + \boldsymbol{\varpi}'\cdot\mathbf{r} =: \varepsilon_0 + \boldsymbol{\varepsilon}_1\cdot\mathbf{r}, \\ \widehat{\mathbf{W}} &= \mathbf{0}, \quad \omega = \psi_0' =: \omega_0. \end{aligned} \tag{22}$$

The functional $\mathcal{H}$ given in (7) simplifies to

$$\begin{aligned} \mathcal{H} = &\int_{\mathcal{I}} (\mathbf{B}_0\cdot\mathbf{v}_0 + \mathbf{B}_1\cdot\mathbf{V} + \Xi_0 w_0 + \boldsymbol{\Xi}_1\cdot\boldsymbol{\varpi} + Q\psi_0) \\ &- \int_{\mathcal{I}} \big(\mathbf{T}'\cdot\mathbf{v}_0 + \big(\mathbf{C}' + \boldsymbol{\Sigma}\big)\cdot\mathbf{V} + N' w_0 + \big(\mathbf{M}' + \mathbf{T}\big)\cdot\boldsymbol{\varpi} + \Delta'\psi_0\big) \\ &+ \int_{\mathcal{B}_b} \big(\mathbf{s} - \hat{\mathbf{f}}\big)\cdot\mathbf{v}_0 + \int_{\mathcal{B}_b} \big[\big(\mathbf{s} - \hat{\mathbf{f}}\big)\otimes\mathbf{r}\big]\cdot\mathbf{V} + \int_{\mathcal{B}_b} (\sigma - \varphi) w_0 \\ &+ \int_{\mathcal{B}_b} [(\sigma - \varphi)\mathbf{r}]\cdot\boldsymbol{\varpi} + \int_{\mathcal{B}_\beta} (\delta - \chi)\psi_0 + \mathcal{R}(\widehat{\mathbf{S}}, \mathbf{s}, \sigma, \widehat{\mathbf{D}}, \delta), \end{aligned} \tag{23}$$

where

$$
\begin{aligned}
\mathbf{B}_0 &= \int_{\mathcal{S}} \hat{\mathbf{b}} + \int_{\partial\mathcal{S}} \hat{\mathbf{f}}, & \mathbf{B}_1 &= \int_{\mathcal{S}} \hat{\mathbf{b}} \otimes \mathbf{r} + \int_{\partial\mathcal{S}} \hat{\mathbf{f}} \otimes \mathbf{r},\\
\mathbf{F}_0 &= \int_{\mathcal{S}} \hat{\mathbf{f}}, & \mathbf{F}_1 &= \int_{\mathcal{S}} \hat{\mathbf{f}} \otimes \mathbf{r},\\
\Xi_0 &= \int_{\mathcal{S}} \beta + \int_{\partial\mathcal{S}} \varphi, & \boldsymbol{\Xi}_1 &= \int_{\mathcal{S}} \beta\mathbf{r} + \int_{\partial\mathcal{S}} \varphi\mathbf{r},\\
\Phi_0 &= \int_{\mathcal{S}} \varphi, & \Phi_1 &= \int_{\mathcal{S}} \varphi\mathbf{r},\\
Q &= \int_{\mathcal{S}} q + \int_{\partial\mathcal{S}} \chi, & X &= \int_{\mathcal{S}} \chi,\\
N &= \int_{\mathcal{S}} \sigma, & \mathbf{M} &= \int_{\mathcal{S}} \sigma\mathbf{r}, & \mathbf{T} &= \int_{\mathcal{S}} \mathbf{s},\\
\mathbf{C} &= \int_{\mathcal{S}} \mathbf{s} \otimes \mathbf{r}, & \boldsymbol{\Sigma} &= \int_{\mathcal{S}} \widehat{\mathbf{S}}, & \Delta &= \int_{\mathcal{S}} \delta.
\end{aligned}
\tag{24}
$$

Note that $\mathcal{R}(\widehat{\mathbf{S}}, \mathbf{s}, \sigma, \widehat{\mathbf{D}}, \delta)$ does not depend upon the displacements and the electric potential. By taking the variation of $\mathcal{H}$ with respect to $\mathbf{v}_0$, $\mathbf{V}$, w_0, $\boldsymbol{\varpi}$ and ψ_0, we obtain

$$
\begin{aligned}
&\mathbf{T}' + \mathbf{B}_0 = \mathbf{0}, \quad \mathbf{C}' + \boldsymbol{\Sigma} + \mathbf{B}_1 = \mathbf{0}, \quad N' + \Xi_0 = 0, \quad \text{on } \mathcal{l},\\
&\mathbf{M}' + \mathbf{T} + \boldsymbol{\Xi}_1 = \mathbf{0}, \quad \Delta' + Q = 0, \quad \text{on } \mathcal{l},
\end{aligned}
\tag{25}
$$

and

$$
\begin{aligned}
&\int_{\mathcal{B}_b} \left(\mathbf{s} - \hat{\mathbf{f}}\right) = \mathbf{0}, & &\int_{\mathcal{B}_b} \left(\mathbf{s} - \hat{\mathbf{f}}\right) \otimes \mathbf{r} = \mathbf{0},\\
&\int_{\mathcal{B}_b} (\sigma - \varphi) = 0, & &\int_{\mathcal{B}_b} (\sigma - \varphi)\mathbf{r} = \mathbf{0}, & &\int_{\mathcal{B}_\beta} (\delta - \chi) = 0.
\end{aligned}
\tag{26}
$$

Here $\mathbf{T}$ is the shear force on a cross-section and $\mathbf{B}_0$ the in-plane body force per unit length. The skew-symmetric part of the 2×2 matrix $\mathbf{C}$ represents the torsional moment and its symmetric part the moment of double forces. The 2×2 symmetric matrix $\boldsymbol{\Sigma}$ gives the in-plane double forces, the skew-symmetric part of the 2×2 matrix $\mathbf{B}_1$ equals the applied torque per unit length, and the symmetric part of $\mathbf{B}_1$ equals the double force/length. The total axial force on a cross-section and the axial body force/length are represented by N and Ξ_0 respectively. Furthermore, $\mathbf{M}$ is the bending moment, $\boldsymbol{\Xi}_1$ the applied bending moment/length, Δ the resultant axial electric displacement, and Q the resultant applied charge per unit length. For $\mathcal{B}_a = \emptyset$, the boundary conditions $(26)_1$ and $(26)_2$ can be expressed in terms of resultant fields defined on the end faces of the rod, a similar remark applies to the case when $\mathcal{B}_\alpha = \emptyset$. Equations (26) describe the boundary conditions on that part of the end faces where mechanical and electric displacements are not prescribed. For $\mathcal{B}_b = \mathcal{B}$, and $\mathcal{B}_\beta = \mathcal{B}$, these equations will give boundary conditions for $\mathbf{T}$, $\mathbf{C}$, N, $\mathbf{M}$ and Δ.

In order for the rod theory to mimic the plate theory developed above, we must choose $\widehat{\mathbf{S}}$, $\mathbf{s}$ and $\widehat{\mathbf{D}}$ such that

$$\widehat{\mathbf{S}}\boldsymbol{\nu} = \hat{\mathbf{f}}, \quad \mathbf{s}\cdot\boldsymbol{\nu} = \varphi, \quad \widehat{\mathbf{D}}\cdot\boldsymbol{\nu} = \chi \quad \text{on } \partial\mathcal{S}. \tag{27}$$

This requires that $\widehat{\mathbf{S}}$, $\mathbf{s}$ and $\widehat{\mathbf{D}}$ be functions of $\mathbf{r}$, the shape of the cross-section, and the distributions of $\hat{\mathbf{f}}$, φ and χ on the boundary of a cross-section. Note that the effects of $\hat{\mathbf{f}}$, φ and χ are included in the balance equations (25) through $\mathbf{B}_0$, $\mathbf{B}_1$, Ξ_0, $\boldsymbol{\Xi}_1$, Φ_0, Φ_1, Q and X. Here we assume that $\widehat{\mathbf{S}}$, $\mathbf{s}$, σ, $\widehat{\mathbf{D}}$ and δ are polynomials in $\mathbf{r}$. For a rod made of a linear elastic material, σ and ε, and δ and ω must be polynomials of the same degree in $\mathbf{r}$. However, the degree of polynomials of $\widehat{\mathbf{S}}$, $\mathbf{s}$ and $\widehat{\mathbf{D}}$ needs to be determined so that $(24)_{11}$–$(24)_{16}$ and the following boundary conditions (28) on $\partial\mathcal{S}$ are satisfied:

$$\int_{\partial\mathcal{S}} \widehat{\mathbf{S}}\boldsymbol{\nu} = \mathbf{0}, \qquad \int_{\partial\mathcal{S}} \mathbf{s}\cdot\boldsymbol{\nu} = 0, \qquad \int_{\partial\mathcal{S}} \widehat{\mathbf{D}}\cdot\boldsymbol{\nu} = 0. \tag{28}$$

Equations $(28)_1$ and $(28)_2$ imply that the resultant of tractions acting on the boundary of every cross-section of the rod vanishes. Similarly, the resultant of normal electric displacement on the boundary of a cross-section of the rod is null. In order for equation $(28)_2$ to be satisfied, $\mathbf{s}$ must be a polynomial of degree 5 in $\mathbf{r}$. However, most classical rod theories assume that $\mathbf{s}$ is an affine function of $\mathbf{r}$ and ignore boundary condition $(28)_2$. We discuss the classical choice below, and the other one in the Appendix. We take

$$\begin{aligned}
\widehat{\mathbf{S}}(\mathbf{r},\zeta) &= \frac{\boldsymbol{\Sigma}(\zeta)}{A},\\
\mathbf{s}(\mathbf{r},\zeta) &= \frac{\mathbf{T}(\zeta)}{A} + \mathbf{C}(\zeta)\mathbf{J}^{-1}\mathbf{r},\\
\sigma(\mathbf{r},\zeta) &= \frac{N(\zeta)}{A} + \mathbf{J}^{-1}\mathbf{r}\cdot\mathbf{M}(\zeta),\\
\widehat{\mathbf{D}}(\mathbf{r},\zeta) &= \mathbf{0}, \qquad \delta(\mathbf{r},\zeta) = \frac{\Delta(\zeta)}{A},
\end{aligned} \tag{29}$$

where A is the area of cross-section and

$$\mathbf{J} = \int_{\mathcal{S}} \mathbf{r}\otimes\mathbf{r} \tag{30}$$

is the inertia tensor.

The variation of $\mathcal{H}$ with respect to $\boldsymbol{\Sigma}$, $\mathbf{T}$, N, Δ, $\mathbf{M}$ and $\mathbf{C}$ gives

$$\begin{aligned}
\begin{Bmatrix} \widehat{\mathbf{E}}_0 \\ \boldsymbol{\gamma}_0 \\ \varepsilon_0 \\ \omega_0 \end{Bmatrix} &= \frac{1}{A}\begin{bmatrix} \mathbb{F}_{ES} & \mathbb{F}_{Es} & \mathbb{F}_{E\sigma} & \mathbb{M}_{E\delta} \\ * & \mathbb{F}_{\gamma s} & \mathbb{F}_{\gamma\sigma} & \mathbb{M}_{\gamma\delta} \\ * & * & \mathbb{F}_{\varepsilon\sigma} & \mathbb{M}_{\varepsilon\delta} \\ -* & -* & -* & \mathbb{N}_{W\delta} \end{bmatrix}\begin{Bmatrix} \boldsymbol{\Sigma} \\ \mathbf{T} \\ N \\ \Delta \end{Bmatrix},\\
\boldsymbol{\varepsilon}_1 &= \mathbf{J}^{-1}\mathbb{F}_{\varepsilon\sigma}\mathbf{M} + \mathbf{J}^{-1}\mathbf{C}^{\mathrm{T}}\mathbb{F}_{\gamma\sigma},\\
\boldsymbol{\Gamma} &= \mathbb{F}_{\gamma s}\mathbf{C}\mathbf{J}^{-1} + (\mathbb{F}_{\gamma\sigma}\otimes\mathbf{M})\mathbf{J}^{-1},
\end{aligned} \tag{31}$$

and

$$\begin{aligned} &\int_{\mathcal{B}_a} \left(\mathbf{v}_0 - \bar{\mathbf{v}}\right) = \mathbf{0}, \qquad \int_{\mathcal{B}_a} \left(\mathbf{V} - \mathbf{J}^{-1}\bar{\mathbf{v}} \otimes \mathbf{r}\right) = \mathbf{0}, \\ &\int_{\mathcal{B}_a} \left(w_0 - \bar{w}\right) = 0, \qquad \int_{\mathcal{B}_a} \left(\boldsymbol{\varpi} - \bar{w}\mathbf{r}\right) = \mathbf{0}, \qquad \int_{\mathcal{B}_\alpha} \left(\psi_0 - \bar{\psi}\right) = 0. \end{aligned} \tag{32}$$

Balance laws (25), constitutive relations (31), boundary conditions (26) and (32), and congruence relations (22) form a complete set of equations for a rod problem. Note that there is no constitutive coupling between the two groups of fields $(\boldsymbol{\Sigma}, \mathbf{T}, N, \Delta)$ and $(\mathbf{M}, \mathbf{C})$. However, they are coupled through the balance laws (25). For $\mathcal{B}_b = \emptyset$ and $\mathcal{B}_\beta = \emptyset$, equations (32) reduce to boundary conditions for $\mathbf{v}_0$, $\mathbf{V}$, w_0, $\boldsymbol{\varpi}$ and ψ_0.

5. Examples

5.1. PLATE-LIKE BODY

5.1.1. *Bending Rigidities of a Transversely Isotropic Plate*

We consider transversely isotropic bodies with the axis of transverse isotropy along the unit vector **a**, and calculate the bending and torsional rigidities of a plate as a function of the angle θ between the unit vectors **a** and **e**. Recall that the unit vector **e** is along the normal to the midsurface of the plate. For simplicity we use rectangular Cartesian coordinate axes with the x_3-axis coincident with the unit vector **e** or the transverse direction, the vector **a** in the $(x_1$–$x_3)$-plane and surfaces $\mathcal{S}^+$ and $\mathcal{S}^-$ free of surface tractions and surface charges. The inversion of equation $(16)_2$ gives **M** and **C** in terms of $\widehat{\mathbf{E}}_1$ and $\boldsymbol{\gamma}_1$. When **a** is parallel to **e**, the matrix $\mathbb{F}$ has the following representation:

$$[\mathbb{F}] = \begin{bmatrix} -\dfrac{1}{E_1} & 0 & -\dfrac{\nu_{12}}{E_1} & 0 & 0 & -\dfrac{\nu_{13}}{E_3} \\ 0 & \dfrac{(1+\nu_{12})}{E_1} & 0 & 0 & 0 & 0 \\ -\dfrac{\nu_{12}}{E_1} & 0 & \dfrac{1}{E_1} & 0 & 0 & -\dfrac{\nu_{13}}{E_3} \\ 0 & 0 & 0 & \dfrac{1}{G_{13}} & 0 & 0 \\ 0 & 0 & 0 & 0 & \dfrac{1}{G_{13}} & 0 \\ -\dfrac{\nu_{13}}{E_3} & 0 & -\dfrac{\nu_{13}}{E_3} & 0 & 0 & \dfrac{1}{E_3} \end{bmatrix}. \tag{33}$$

Here E_1, E_2 and E_3 are the Young's moduli along the principal material axes, ν_{13} and G_{13} are the Poisson's ratio and the shear modulus, respectively. When **a** is

parallel to **e**, the principal material axes coincide with the coordinate axes. The 2×2 symmetric matrix $\widehat{\mathbf{E}}$ has been written as a 3×1 matrix with entries $\widehat{E}_{11}$, $\widehat{E}_{12}$ and $\widehat{E}_{22}$ in columns 1, 2 and 3, respectively. When the unit vector **a** is not parallel to the unit vector **e**, i.e., **a** is not in the transverse direction, then the elements of the 3×3 matrix $\mathbb{F}$ are functions of $\cos\theta$, $\sin\theta$, E_1, E_3, ν_{12}, ν_{13} and G_{13}, and

$$\begin{aligned}\mathbb{F}(\mathbf{S}) = {} & \alpha_1 \mathbf{I}_\pi \mathbf{S} \mathbf{I}_\pi + \alpha_2 (\mathbf{I}_\pi \cdot \mathbf{S}) \mathbf{I}_\pi + \alpha_3 (\mathbf{P}\mathbf{S} + \mathbf{S}\mathbf{P}) \\ & + \alpha_4 (\operatorname{tr}(\mathbf{S})\mathbf{P} + (\mathbf{P} \cdot \mathbf{S})\mathbf{I}) + \alpha_5 (\mathbf{P} \cdot \mathbf{S})\mathbf{P},\end{aligned} \tag{34}$$

where $\mathbf{P} = \mathbf{a} \otimes \mathbf{a}$, $\mathbf{I}_\pi = \mathbf{I} - \mathbf{P}$, $\mathbf{I}$ is the identity matrix, and

$$\begin{aligned}&\alpha_1 = \frac{1 + \nu_{12}}{E_1}, \qquad \alpha_2 = -\frac{\nu_{12}}{E_1}, \qquad \alpha_3 = \frac{1}{G_{13}}, \qquad \alpha_4 = -\frac{\nu_{13}}{E_3}, \\ &\alpha_5 = \frac{G_{13} - 2E_3 + 2G_{13}\nu_{13}}{G_{13}E_3}.\end{aligned} \tag{35}$$

Writing

$$M_{11} = J\widehat{E}_{11} f(E_1,\ E_3,\ \nu_{12},\ \nu_{13},\ G_{13},\ \theta), \quad J = \frac{2}{3}h^3, \tag{36}$$

we have plotted in Figure 1 the normalized f, i.e., $f(\theta)/f(0)$, as a function of θ for $E_3/E_1 = \eta = 0.3,\ 0.5$ and 0.9, and $\nu_{12} = \nu_{13} = 0.3$, $G_{13} = E_1/2(1 + \nu_{13})$. It is clear that for η far away from 1.0, $f(\theta)$ depends strongly upon θ because of the inclusion in the plate model of double forces without moments. For $\theta = 0$, the flexural rigidities D_{11}, D_{22} and D_{12} and the torsional rigidity G_{12} are given by

$$D_{11} = D_{22} = \frac{JE_1}{(1 - \nu_{12}^2)}, \qquad D_{12} = \frac{JE_1\nu_{12}}{1 - \nu_{12}^2}, \qquad G_{12} = \frac{JE_1}{1 + \nu_{12}}, \tag{37}$$

and for $\theta = 90^\circ$,

$$\begin{aligned}&D_{11} = \frac{JE_3^2}{(E_3 - E_1\nu_{13}^2)}, \qquad D_{22} = \frac{JE_1E_3}{(E_3 - E_1\nu_{13}^2)}, \\ &D_{12} = \nu_{13}D_{22}, \qquad G_{12} = JG_{13}.\end{aligned} \tag{38}$$

Figure 2 depicts the value of θ as a function of η for which D_{11} is maximum. For a rather large range of values of η, the value of θ that optimizes D_{11} varies between 30° and 34°. For $\theta \neq 0$, several components of the 3×3 flexural rigidity matrix are nonvanishing.

5.1.2. *Cylindrical Deformations of a Transversely Isotropic Plate*

We now use equations (13) to analyze cylindrical deformations of a homogeneous transversely isotropic plate with only equal and opposite charges applied to the top and bottom surfaces. The plate is assumed to be infinite in one of the in-plane directions, and either both edges are clamped and grounded, or one edge is clamped

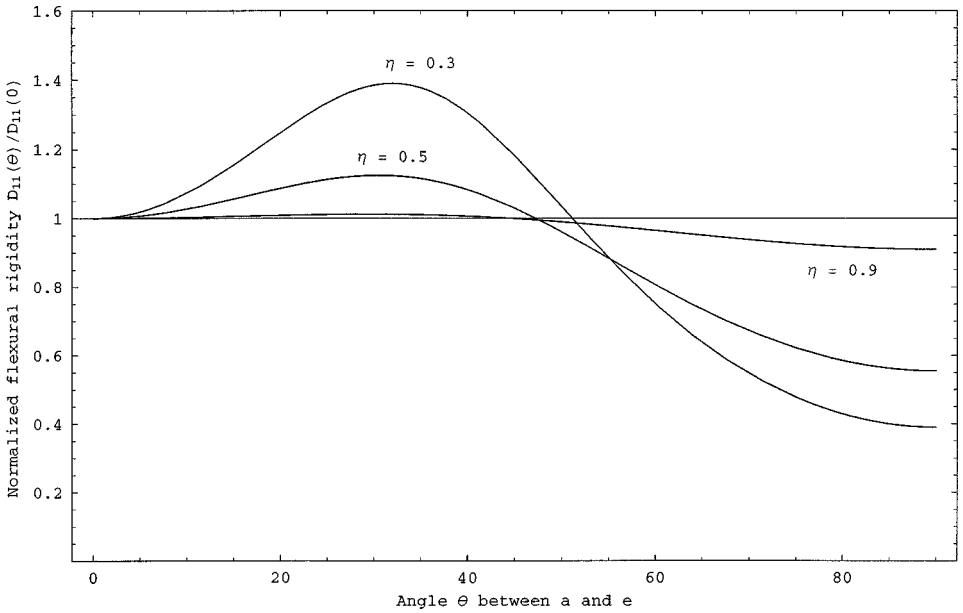

Figure 1. Normalized bending rigidity D_{11} vs. the angle θ between the axis of transverse isotropy and the normal to the midsurface of the plate.

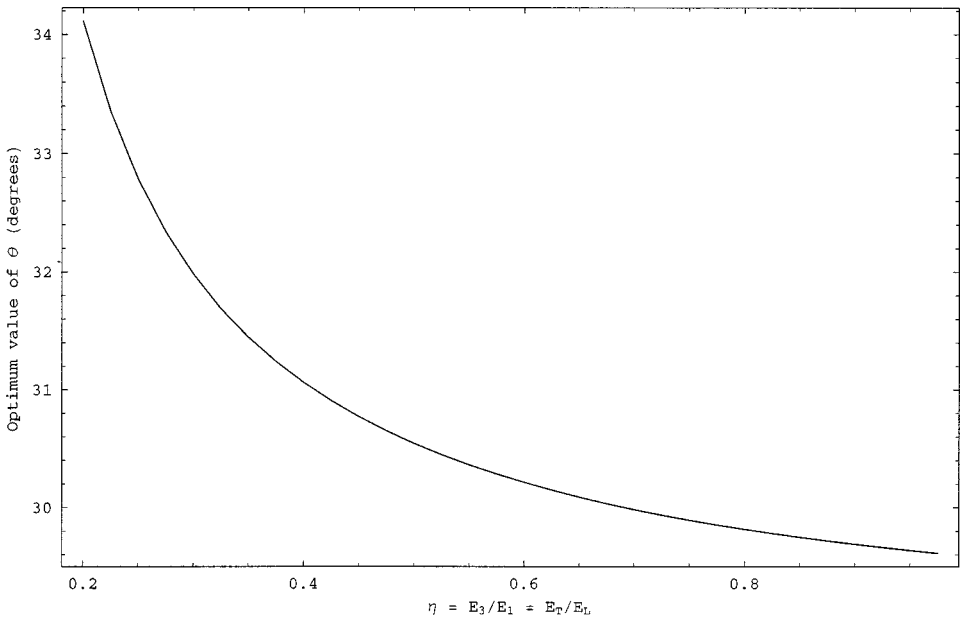

Figure 2. Optimum value of the angle θ between the axis of transverse isotropy and the normal to the midsurface of the plate.

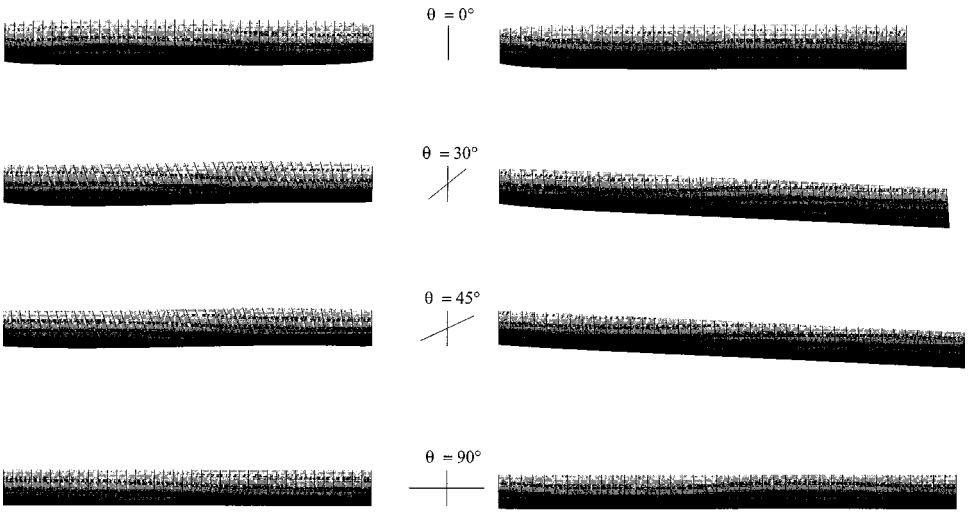

Figure 3. Deformed shapes, for $\theta = 0°$, 30°, 45° and 90°, of the clamped–clamped and the clamped-free plate subjected to equal and opposite charges on the top and bottom surfaces.

and grounded and the other is mechanically and electrically free. There are no body forces and body charges. For this problem, equations (9) simplify to

$$\begin{aligned} v(r,\zeta) &= v_0(r) + \zeta v_1(r), \qquad w(r,\zeta) = w_0(r) + \zeta w_1(r), \\ \psi(r,\zeta) &= \psi_0(r) + \zeta \psi_1(r), \end{aligned} \tag{39}$$

where r is the distance measured from the clamped edge of the plate. A numerical solution of equations (13), (16), (17), (10) and (39) was found by the finite element method. Values of material parameters used to compute results are given below in equations (48) for $\theta = 45°$; those for $\theta \neq 45°$ can be obtained by using the appropriate transformation rules. For a surface charge density of 10^{12} C/m^2 and the span to thickness ratio of 5 Figure 3 exhibits the deformed shapes of the plates for $\theta = 0$, 30°, 45° and 90°. The vertical lines indicate the deformed normals to the midsurface of the plate. Figures 4–9 depict the variations of v_0, v_1, w_0, w_1, ψ_0' and ψ_1 along the span of the plate. For $\theta = 0°$ and 90° we recover classical results showing coupling between the electrical and the mechanical effects. That is, the thickness of the plate changes and there is no transverse shear deformation of the plate. For $\theta = 30°$ and 45°, there is significant bending and shearing of the plate but the changes in the thickness are small as compared to those for $\theta = 0°$ and 90°. A considerable part of the energy used to change the thickness of the plates for $\theta = 0°$ and 90° is consumed to bend and shear the plates when $\theta = 30°$ and 45°. For $\theta = 30°$ and 45°, the in-plane electric field exhibits a boundary-layer effect near the clamped edges. However, for $\theta = 0°$ and 90°, the in-plane electric field is essentially zero all over the midsurface of the plate. The electric field in the

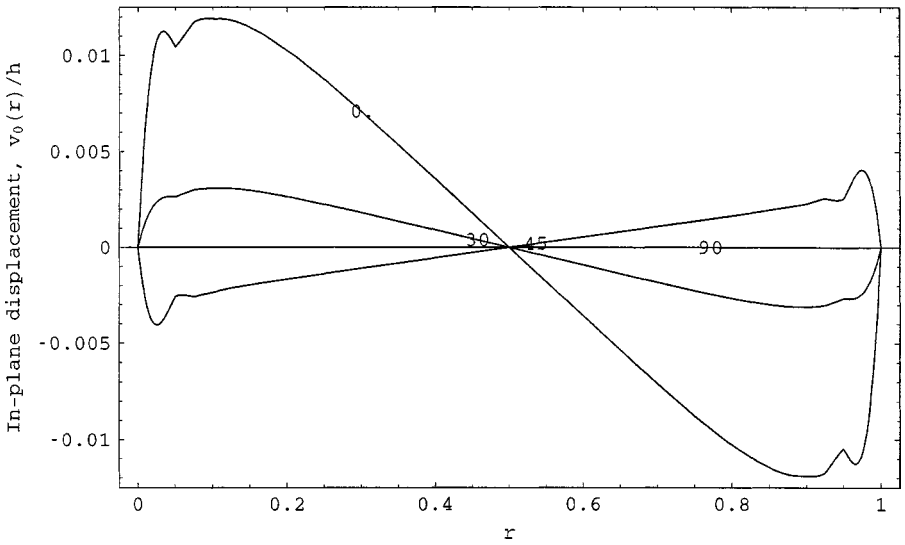

(a)

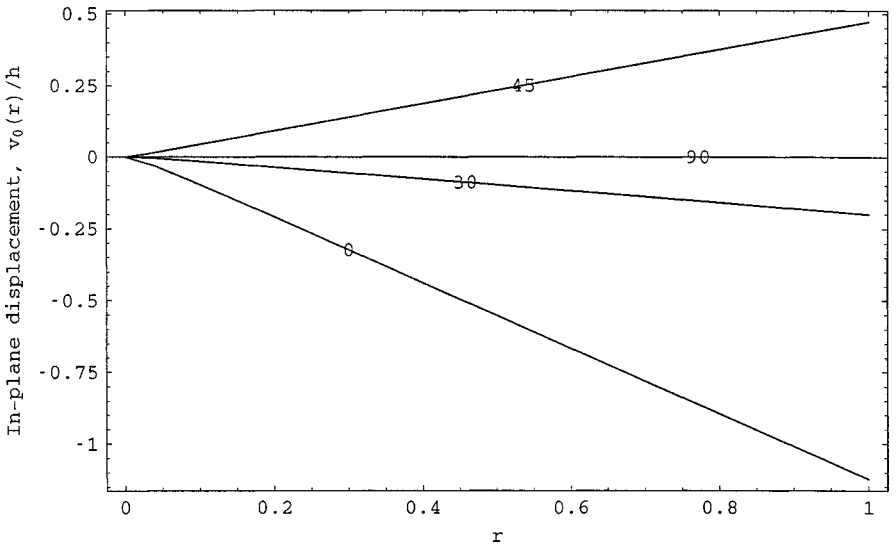

(b)

Figure 4. Variation of the in-plane displacement, v_0, along the span of the plate; (a) clamped–clamped, (b) clamped-free.

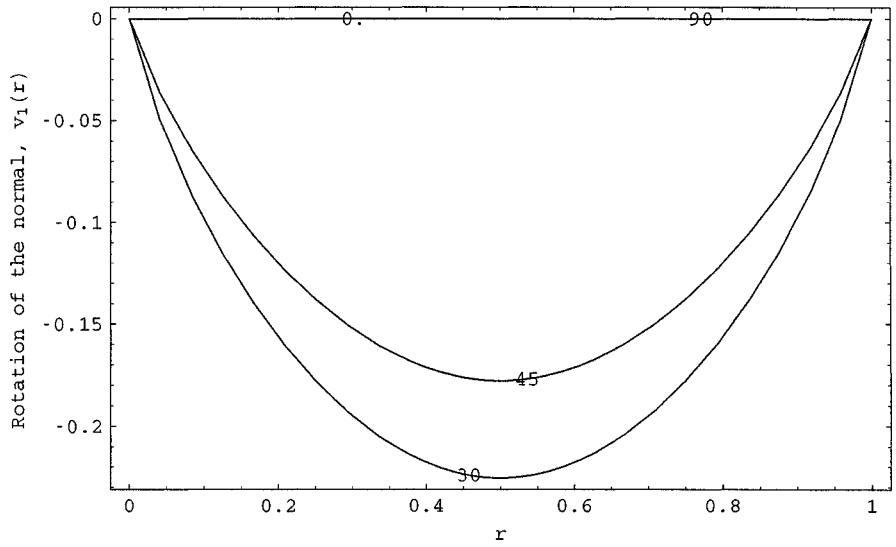

(a)

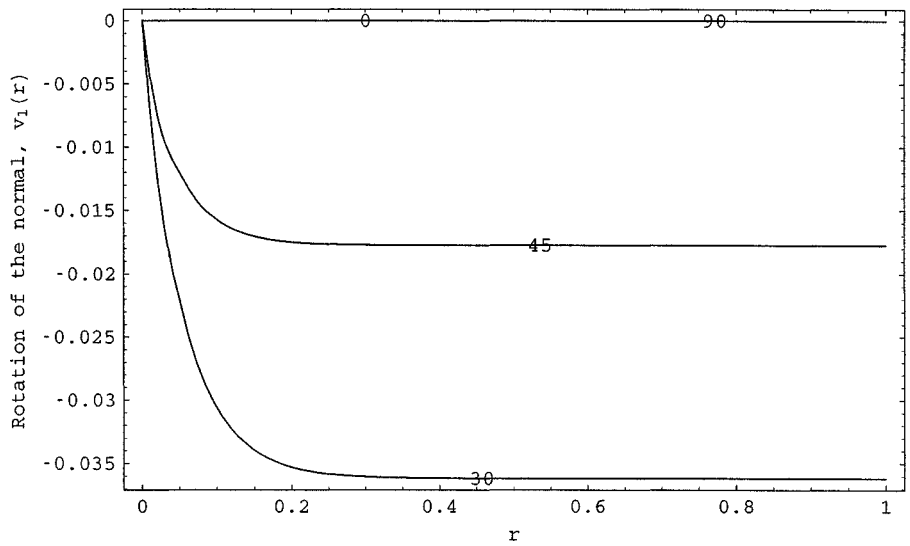

(b)

Figure 5. Variation along the span of the rotation about the long edge of the plate; (a) clamped–clamped, (b) clamped-free.

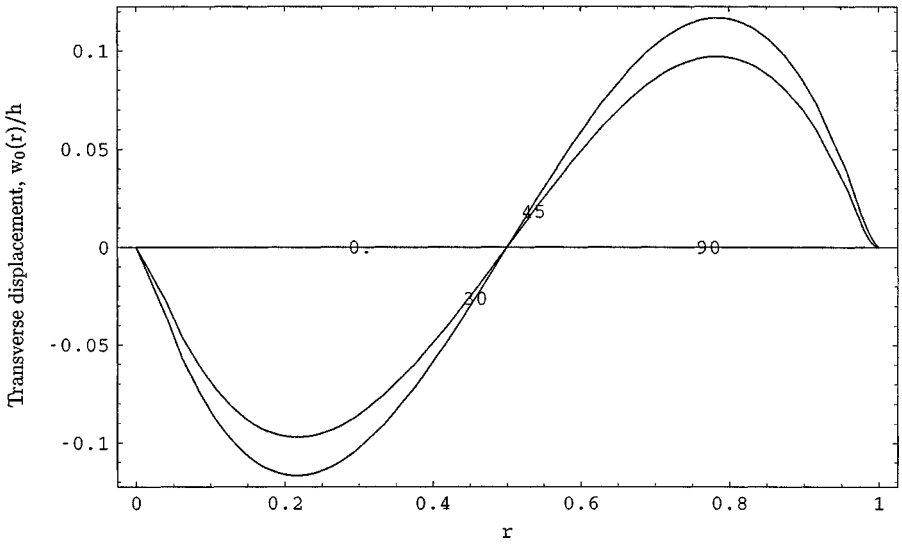

(a)

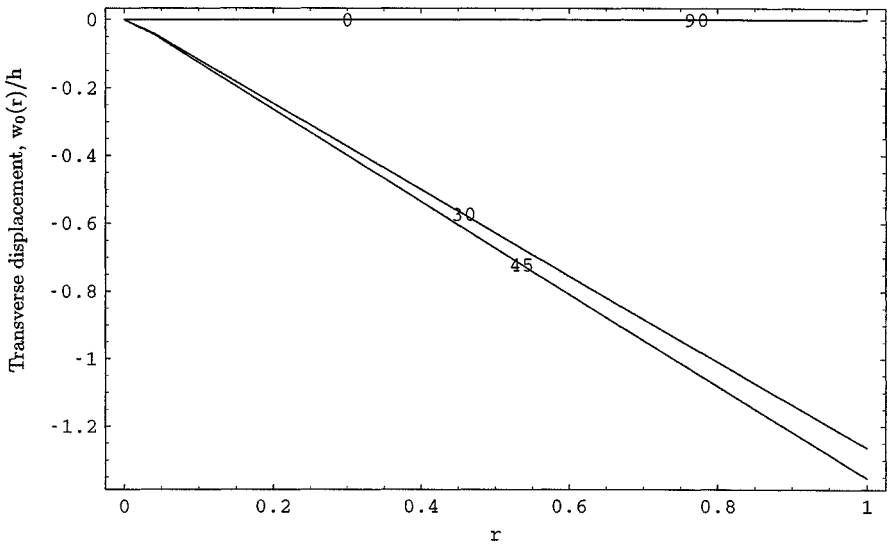

(b)

Figure 6. Variation along the span of the transverse displacement of points on the midsurface of the plate; (a) clamped–clamped, (b) clamped-free.

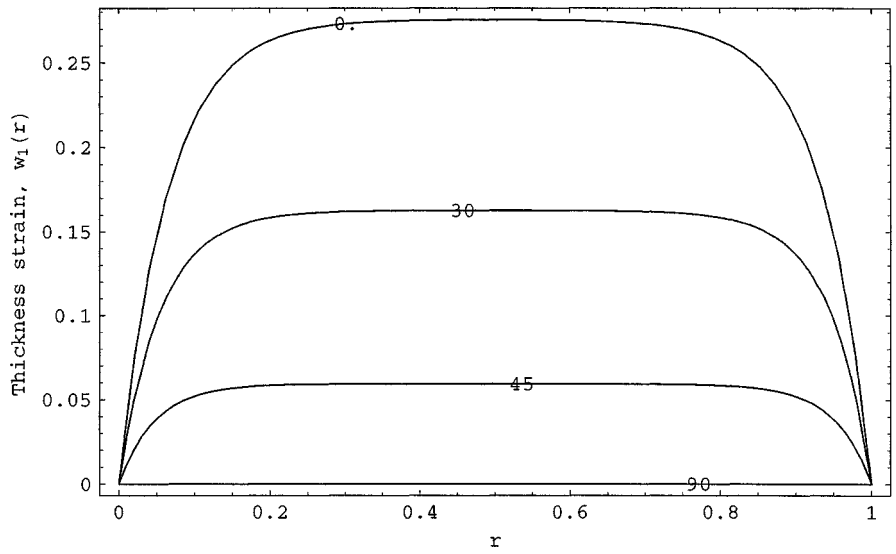

(a)

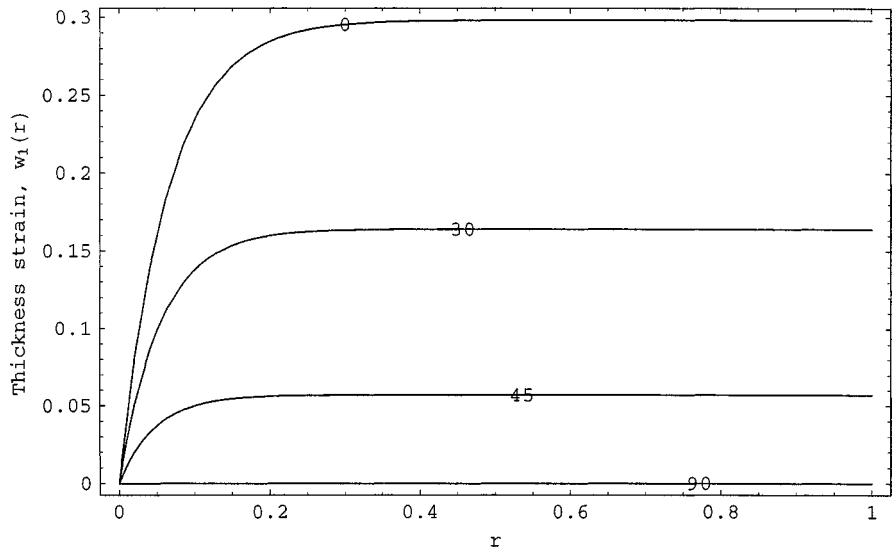

(b)

Figure 7. Variation of the transverse normal strain along the span of the plate; (a) clamped–clamped, (b) clamped-free.

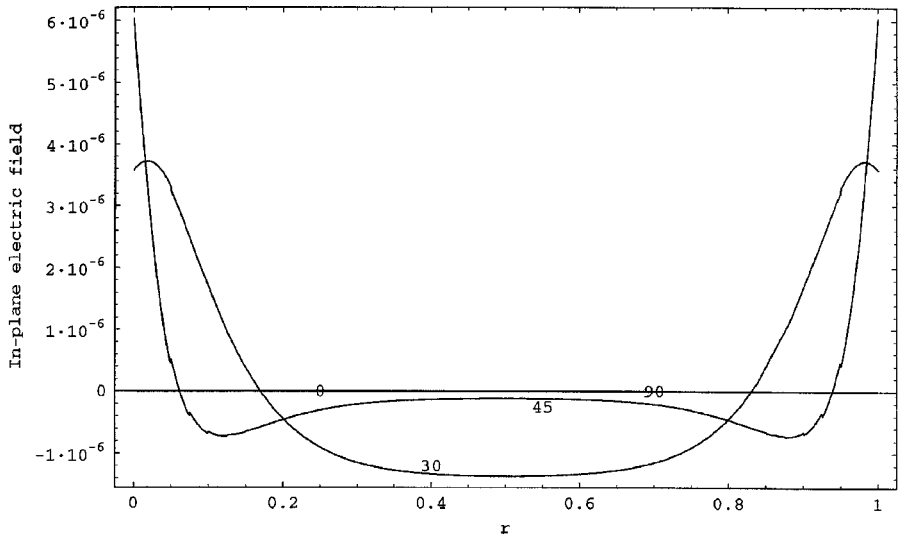

(a)

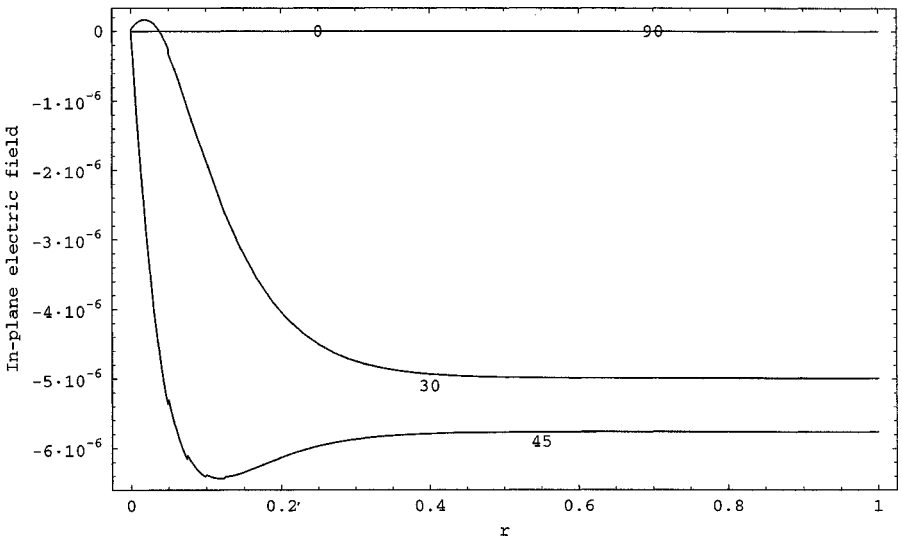

(b)

Figure 8. Variation along the span of the in-plane electric field on the midsurface of the plate; (a) clamped–clamped, (b) clamped-free.

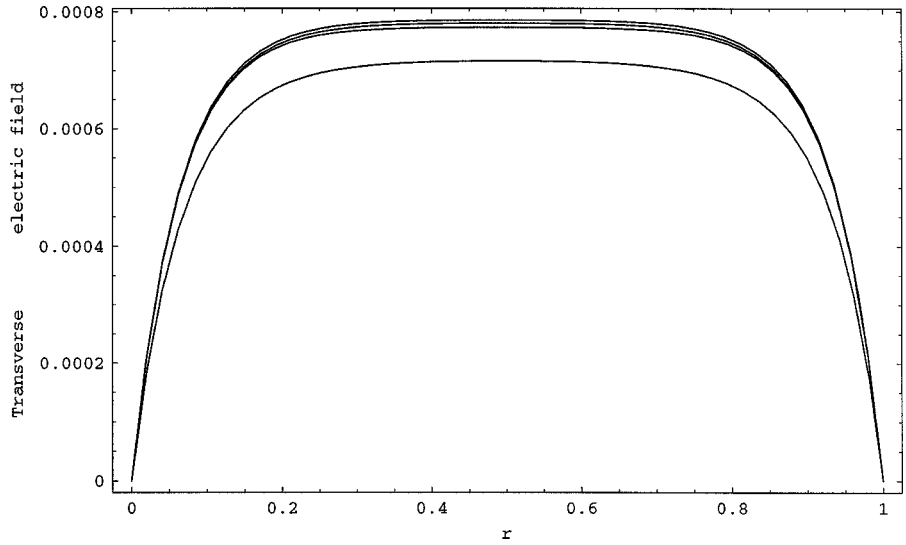

(a)

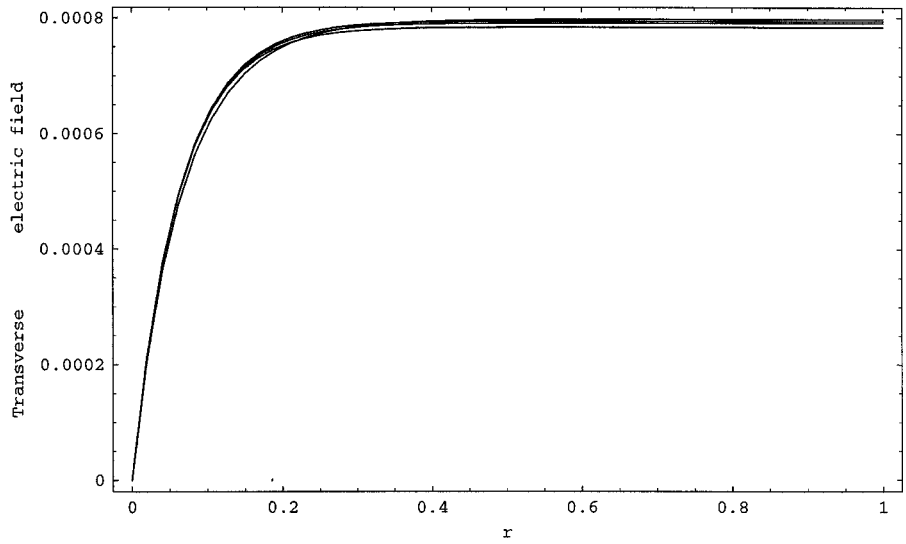

(b)

Figure 9. Variation of the transverse electric field along the span of the plate; (a) clamped–clamped, (b) clamped-free.

thickness direction exhibits a boundary layer effect near the clamped end for all values of θ. There is no boundary layer effect near the free edge of the plate.

5.2. ROD-LIKE BODY

We study electromechanical deformations of a circular cylindrical rod subjected to only electric charges at the end faces. Thus, we set

$$\begin{array}{llll} \mathcal{B}_a = \mathcal{S}^-, & \mathcal{B}_b = \mathcal{S}^+, & \mathcal{B}_\alpha = \mathcal{S}^-, & \mathcal{B}_\beta = \mathcal{S}^+, \\ \hat{\mathbf{b}} = \mathbf{0}, & \beta = 0, & q = 0 & \text{in } \mathcal{P}, \\ \hat{\mathbf{f}} = 0, & \varphi = 0, & \text{on } \mathcal{M} \cup \mathcal{B}_b, \ \chi = 0, & \text{on } \mathcal{M}, \\ \chi = \bar{\chi}, & \text{on } \mathcal{B}_\beta, & & \\ \bar{\mathbf{v}} = \mathbf{0}, & \bar{w} = 0, & \bar{\psi} = 0, & \text{on } \mathcal{S}^-. \end{array} \tag{40}$$

That is, the end face $\mathcal{S}^-$ is rigidly clamped and kept at zero electric potential while the end face $\mathcal{S}^+$ is traction free and carries an electric charge. The mantle of the rod is free of surface tractions and surface charges. Also, the body force and the charge density vanish in $\mathcal{P}$. Corresponding to (40) the boundary conditions become

$$\mathbf{T}(h) = 0, \quad \mathbf{C}(h) = 0, \quad N(h) = 0, \quad \mathbf{M}(h) = 0, \quad \Delta(h) = \int_{\mathcal{S}^+} \bar{\chi} = X. \tag{41}$$

The solution of the equilibrium equations (25) under the boundary conditions (41) for $\mathbf{T}$, N, $\mathbf{M}$ and Δ is

$$\mathbf{T}(\zeta) = \mathbf{0}, \qquad N(\zeta) = 0, \qquad \mathbf{M}(\zeta) = \mathbf{0}, \qquad \Delta(\zeta) = X. \tag{42}$$

However, the fields $\mathbf{C}$ and $\mathbf{\Sigma}$ can not be found from the equilibrium equations $(25)_2$ because the number of unknowns exceeds the number of equations. The constitutive relations (31) and equations (42) give

$$\begin{aligned} \widehat{\mathbf{E}}_0 &= \mathrm{SYM}\mathbf{V} = \frac{1}{A}(\mathbb{F}_{ES}\mathbf{\Sigma} + \mathbb{M}_{E\delta}X), \\ \mathbf{\Gamma} &= \mathbf{V}' = \mathbb{F}_{\gamma s}\mathbf{C}\mathbf{J}^{-1} \end{aligned} \tag{43}$$

which when substituted in $(25)_2$ with $\mathbf{B}_1 = \mathbf{0}$, and in $(26)_2$, yield the following equations for the determination of $\mathbf{V}$:

$$\left(\mathbb{F}_{\gamma s}^{-1}\mathbf{V}'\mathbf{J}\right)' + A\mathbb{F}_{ES}^{-1}\mathrm{SYM}\mathbf{V} = \mathbb{F}_{ES}^{-1}\mathbb{M}_{E\delta}X, \qquad \mathbf{V}'(h) = 0, \qquad \mathbf{V}(-h) = \mathbf{0}. \tag{44}$$

Equation $(44)_3$ follows from $(32)_2$.

We now assume that the rod is of uniform circular cross-section, the material properties do not vary in the axial direction, $\mathbf{J}$ is the spherical tensor, $\mathbf{J} = j\widehat{\mathbf{I}}$, and introduce the non-dimensionalization $x = (\zeta + h)/2h$. Here $\widehat{\mathbf{I}}$ is the 2×2 identity tensor. With these assumptions, equations (44) become

$$\mathbf{V}^{**} + \frac{4Ah^2}{j}\mathbb{F}_{\gamma s}\mathbb{F}_{ES}^{-1}\mathrm{SYM}\mathbf{V} = \frac{4h^2}{j}\mathbb{F}_{\gamma s}\mathbb{F}_{ES}^{-1}\mathbb{M}_{E\delta}X, \quad \mathbf{V}(0) = 0, \quad \mathbf{V}^*(1) = 0, \tag{45}$$

where * (not to be confused with $*$ in (6)) denotes the derivative with respect to x. Knowing $\mathbf{V}$, and using equations (22) and (31), we can find fields $\boldsymbol{\varpi}$, $\mathbf{v}_0$, w_0 and ψ_0 from

$$\begin{aligned}
\boldsymbol{\varpi}(x) &= \mathbf{V}^{\mathrm{T}}(x)\mathbb{F}_{\gamma s}^{-1}\mathbb{F}_{\gamma\sigma},\\
\mathbf{v}_0(x) &= \int_0^x \left[\mathbb{F}_{Es}^{\mathrm{T}}\mathbb{F}_{ES}^{-1}\mathrm{SYM}\mathbf{V}(\xi) - \mathbf{V}^{\mathrm{T}}(\xi)\mathbb{F}_{\gamma s}^{-1}\mathbb{F}_{\gamma\sigma}\right.\\
&\quad \left. + \frac{1}{A}\big(\mathbb{M}_{\gamma\delta} - \mathbb{F}_{Es}^{\mathrm{T}}\mathbb{F}_{ES}^{-1}\mathbb{M}_{E\delta}\big)X\right]\mathrm{d}\xi,\\
w_0(x) &= \int_0^x \left[\mathbb{F}_{E\sigma}^{\mathrm{T}}\mathbb{F}_{ES}^{-1}\mathrm{SYM}\mathbf{V}(\xi) + \frac{1}{A}\big(\mathbb{M}_{\varepsilon\delta} - \mathbb{F}_{E\sigma}^{\mathrm{T}}\mathbb{F}_{ES}^{-1}\mathbb{M}_{E\delta}\big)X\right]\mathrm{d}\xi,\\
\psi_0(x) &= \int_0^x \left[\frac{1}{A}\big(\mathbb{N}_{\omega\delta} + \mathbb{M}_{E\delta}^{\mathrm{T}}\mathbb{F}_{ES}^{-1}\mathbb{M}_{E\delta}\big)X - \mathbb{M}_{E\delta}^{\mathrm{T}}\mathbb{F}_{ES}^{-1}\mathrm{SYM}\mathbf{V}(\xi)\right]\mathrm{d}\xi.
\end{aligned} \tag{46}$$

Using the following representation for $\mathbf{V}$

$$[\mathbf{V}] = V_0\begin{bmatrix}1 & 0\\ 0 & -1\end{bmatrix} + V_1\begin{bmatrix}1 & 0\\ 0 & 1\end{bmatrix} + V_t\begin{bmatrix}0 & 1\\ 1 & 0\end{bmatrix} + V_x\begin{bmatrix}0 & 1\\ -1 & 0\end{bmatrix}, \tag{47}$$

for a circular rod, we have plotted in Figure 10 the variation of V_0, V_1, V_x and V_t with $x \in [0, 1]$. The wavelengths of V_x and V_t depend upon the angle between the centroidal axis of the bar and the axis of transverse isotropy, and also on the aspect ratio (i.e., diameter of the cross-section/length of the bar). In order to plot results in Figure 10, various material (PZT-5) and geometric parameters were assigned the following values in MKS units (e.g., see [16])

$$[\mathbb{F}] = 10^{-12} \times \begin{bmatrix}
24.299 & 0 & -5.32533 & -11.8846 & 0 & -0.925055\\
0 & 34.762 & 0 & 0 & 9.53798 & 0\\
-5.32533 & 0 & 14.4336 & -4.76207 & 0 & -5.32533\\
-5.9423 & 0 & -2.38104 & 29.2625 & 0 & -5.9423\\
0 & 9.53798 & 0 & 0 & 34.762 & 0\\
-0.925055 & 0 & -5.32533 & -11.8846 & 0 & 24.299
\end{bmatrix},$$

$$[\mathbb{M}] = 10^{-18}\begin{bmatrix}
-4750 & -38100 & 4750\\
-19100 & 0 & -19100\\
8080 & 0 & -8080\\
12800 & 0 & -12800\\
19100 & 0 & 19100\\
-4750 & 38100 & 4750
\end{bmatrix}, \tag{48}$$

$$[\mathbb{N}] = 10^{-18}\begin{bmatrix}
65.9 & 0 & -0.576\\
0 & 65.3 & 0\\
-0.576 & 0 & 65.9
\end{bmatrix}$$

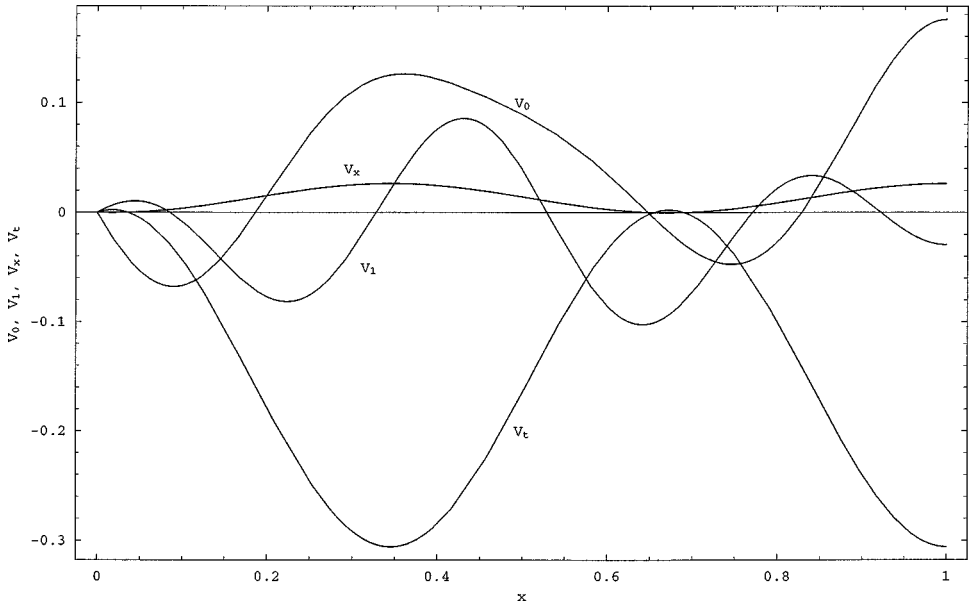

Figure 10. Variation of the twisting and in-plane deformations of a cross-section of the rod along its centroidal axis.

- aspect ratio $= 0.4$,
- angle between the centroidal axis and the axis of transverse isotropy $= 45^\circ$,
- total charge applied at one end face $= 10^{12}$.

In the representation (47) of $\mathbf{V}$, the deformation $\mathbf{V}_0$ transforms a circle into an ellipse, $\mathbf{V}_1$ is a spherical deformation or dilatation of the cross-section, $\mathbf{V}_t$ accounts for the shearing deformation of the cross-section, and $\mathbf{V}_x$ gives the twisting of the cross-section. It is clear from the results plotted in Figure 10 that the deformation of the cross-section due to its being twisted is small, and that due to shearing is quite large.

Figure 11 depicts the deformed shapes of the cross-section at twenty locations along the axis of the bar. Due to different deformations of these cross-sections, a prismatic bar is deformed into a non-prismatic one. By varying the material properties along the axis of the bar, one should be able to optimize a desired mode of deformation. These material properties could be varied by changing the symmetry group of the material.

We have plotted in Figure 12 the axial displacement of points on the centroidal axis of the bar. The dotted curve is for the case when each cross-section of the bar is assumed to be rigid, i.e., sym$\mathbf{V} = \mathbf{0}$, and the solid curve for deformable cross-sections. It is clear that the axial displacement of a point increases significantly when deformations of a cross-section are accounted for. The difference between the axial displacements of a point for deformable and rigid cross-sections increases noticeably for points away from the fixed end-face. Thus, the electrostrictive effect

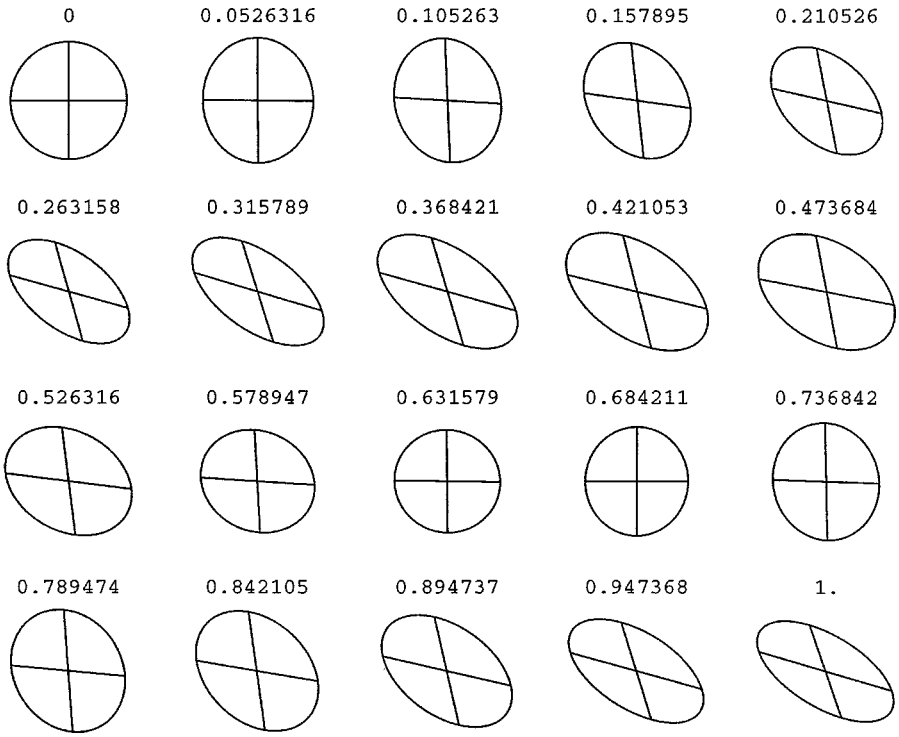

Figure 11. Deformed shapes of a cross-section at different locations on the centroidal axis of the rod.

can be significantly modified by adjusting the angle between the direction **a** of transverse isotropy and the axis **e** of the bar. However, this increase in elongation is accompanied by the simultaneous bending and twisting of the bar.

6. Conclusions

We have derived governing equations, constitutive relations, and boundary conditions for quasistatic deformations of an anisotropic plate-like and an anisotropic rod-like body by using a mixed variational principle of Yang and Batra for a piezoelectric body. The transverse shear deformations of a plate and the changes in its thickness are accounted for. Similarly, deformations of a cross-section of the rod due to double forces without moments applied at its mantle are considered.

We have also computed the bending rigidities of a homogeneous transversely isotropic plate as a function of the angle θ between the axis **a** of transverse isotropy and the unit vector **e** normal to the mid-surface of the plate. It is found that for a large range of the values of E_T/E_L, the value of θ that optimizes D_{LL} varies between 30° and 34°. Here subscripts L and T signify longitudinal and transverse directions, respectively. The plate equations are employed to study the cylindrical

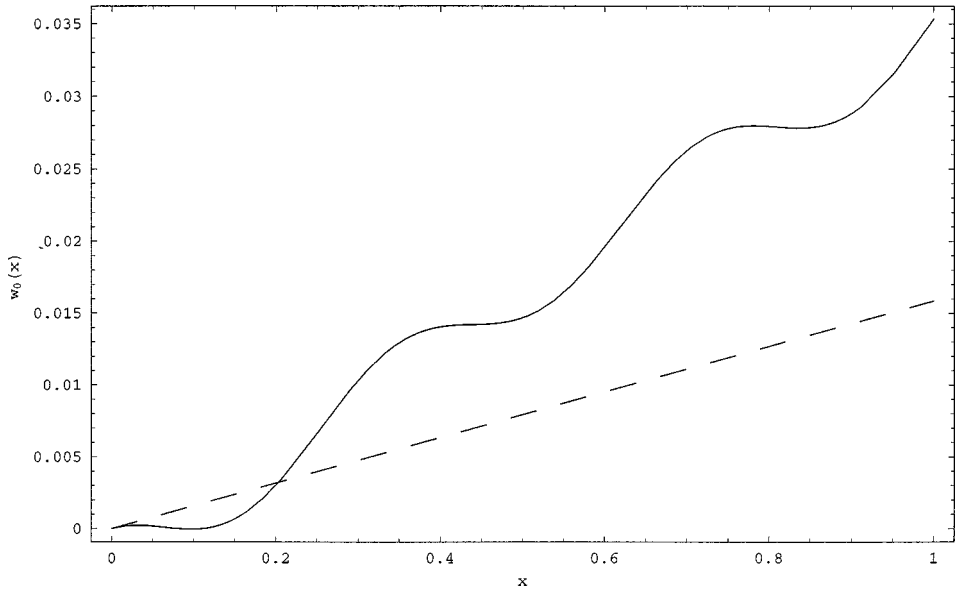

Figure 12. Axial displacements of points on the centroidal axis of the rod.

deformations of a transversely isotropic plate with either both edges clamped and grounded or one edge clamped and grounded and the other mechanically and electrically free. Only electric charges are applied to the top and bottom surfaces of the plate. The angle between the axis of transverse isotropy and the unit normal to the midsurface of the plate strongly influences the transverse deformations of the plate.

We have used the rod equations to analyze deformations of a homogeneous and transversely isotropic bar loaded on one end face by surface charges only with the other end face rigidly clamped and kept at zero electric potential. The mantle of the rod is assumed to be free of surface tractions and surface charges. When the axis of transverse isotropy makes an angle of 45° with the centroidal axis of the rod, the deformations of the cross-section significantly influence the axial elongation of points on the centroidal axis. The axial elongation is simultaneously accompanied by the bending and twisting of the rod.

Acknowledgement

This work was partially supported by the ARO grant DAAG55-98-1-0030 and the NSF grant CMS9713453 to Virginia Polytechnic Institute and State University.

Appendix

The lowest order polynomial in $\mathbf{r}$ that simultaneously satisfies equations $(24)_{14}$ and $(28)_2$ is

$$\begin{aligned}\mathbf{s} \;=\; & \mathbf{s}_0 + \mathbf{C}\big[a_1\mathbf{H}_2\mathbf{r} + a_2\mathbf{H}_3(\mathbf{r}\otimes\mathbf{r}) + a_3\mathbf{H}_4(\mathbf{r}\otimes\mathbf{r}\otimes\mathbf{r}) \\ & + a_4\mathbf{H}_5(\mathbf{r}\otimes\mathbf{r}\otimes\mathbf{r}\otimes\mathbf{r}) + a_5\mathbf{H}_6(\mathbf{r}\otimes\mathbf{r}\otimes\mathbf{r}\otimes\mathbf{r}\otimes\mathbf{r})\big], \end{aligned} \tag{A.1}$$

where $\mathbf{s}_0$ is independent of $\mathbf{r}$,

$$\mathbf{H}_k = \mathbf{J}_k^{-1},\ \mathbf{J}_k = \int_{\mathcal{S}} \underbrace{\mathbf{r}\otimes\mathbf{r}\cdots\otimes\mathbf{r}}_{k \text{ times}},$$

and in rectangular Cartesian coordinates with summation implied on repeated indices,

$$\big[\mathbf{H}_3(\mathbf{r}\otimes\mathbf{r})\big]_i = H_{3ijk}r_jr_k,\ H_{ijkl}J_{jklm} = \delta_{im}. \tag{A.2}$$

Substitution from (A1) into $(24)_{14}$ and $(28)_2$ gives

$$\begin{aligned} & a_1 + a_2 + a_3 + a_4 + a_5 = 1, \\ & a_1\mathrm{tr}\,(\mathbf{C}\mathbf{H}_2) + 3a_3\mathrm{tr}\,(\mathbf{C}\mathbf{H}_4\mathbf{J}_2) + 4a_4\mathrm{tr}\,(\mathbf{C}\mathbf{H}_5\mathbf{J}_3) + 5a_5\mathrm{tr}\,(\mathbf{C}\mathbf{H}_6\mathbf{J}_4) = 0. \end{aligned} \tag{A.3}$$

Equation $(A.3)_2$ yields four equations for four different choices of the 2×2 matrix $\mathbf{C}$ which together with $(A.3)_1$ determine $a_1, a_2, \ldots, a_5$. Setting $\mathbf{s}_0 = \mathbf{T}(\xi)/A$ in (A.1), substituting this expression for $\mathbf{s}$ in $\mathcal{H}$, and taking the variations with respect to $\mathbf{C}$, we obtain

$$\begin{aligned} & \widehat{\mathbf{E}}_0 = \widehat{\mathbf{E}}_{op} + \frac{1}{A}\mathbb{F}_{Es}\mathbf{C}\mathbf{k}, \qquad \boldsymbol{\gamma}_0 = \boldsymbol{\gamma}_{op} + \frac{1}{A}\mathbb{F}_{\gamma s}\mathbf{C}\mathbf{k}, \quad \varepsilon_0 = \varepsilon_{op} + \frac{\mathbb{F}^{\mathrm{T}}_{\gamma\sigma}}{A}\mathbf{C}\mathbf{k}, \\ & \omega_0 = \omega_{op} + \frac{1}{A}\mathbb{M}^{\mathrm{T}}_{\gamma\delta}\mathbf{C}\mathbf{k}, \\ & \varepsilon_1 = \mathbf{J}^{-1}\big(\mathbb{F}_{\varepsilon\sigma}\mathbf{M} + \mathbf{C}^{\mathrm{T}}\mathbb{F}_{\gamma\sigma}\big), \\ & \boldsymbol{\Gamma} = \frac{1}{A}\big(\mathbb{F}^{\mathrm{T}}_{Es}\boldsymbol{\Sigma} + \mathbb{F}_{\gamma s}\mathbf{T} + \mathbb{F}_{\gamma\sigma}N + \mathbb{M}_{\gamma\delta}\Delta\big)\otimes\mathbf{k} \\ & \qquad + (\mathbb{F}_{\gamma\sigma}\otimes\mathbf{M})\mathbf{J}^{-1} + \mathbb{F}_{\gamma s}\mathbf{C}\mathbf{K}, \end{aligned} \tag{A.4}$$

where

$$\mathbf{k} = a_2\mathbf{H}_3\mathbf{J}_2 + a_3\mathbf{H}_4\mathbf{J}_3 + a_4\mathbf{H}_5\mathbf{J}_4 + a_5\mathbf{H}_6\mathbf{J}_5, \tag{A.5}$$

and $\mathbf{K}$ is the following 2×2 matrix:

$$\begin{aligned} \mathbf{K}_{ij} = {} & a_1^2\mathbf{H}_{2ij} + 2a_1(1-a_1)\mathbf{H}_{2ij} \\ & + a_2(a_2\mathbf{H}_{3ihk}\mathbf{J}_{4hklm}\mathbf{H}_{3lmj} + \cdots + a_5\mathbf{H}_{6ihklmn}\mathbf{J}_{7hklmnpq}\mathbf{H}_{3pqj}) \\ & + a_3(a_2\mathbf{H}_{3ihk}\mathbf{J}_{5hklmn}\mathbf{H}_{4lmnj} + \cdots + a_5\mathbf{H}_{6ihklmn}\mathbf{J}_{8hklmnpqr}\mathbf{H}_{4pqrj}) \\ & + a_4(a_2\mathbf{H}_{3ihk}\mathbf{J}_{6hklmnp}\mathbf{H}_{5lmnpj} + \cdots + a_5\mathbf{H}_{6ihklmn}\mathbf{J}_{9hklmnpqrs}\mathbf{H}_{5pqrsj}) \\ & + a_5(a_2\mathbf{H}_{3ihk}\mathbf{J}_{7hklmnpq}\mathbf{H}_{6lmnpqj} + \cdots + a_5\mathbf{H}_{6ihklmn}\mathbf{J}_{10hklmnpqrst}\mathbf{H}_{6pqrstj}). \end{aligned} \tag{A.6}$$

Expressions for $\widehat{\mathbf{E}}_{op}$, $\boldsymbol{\gamma}_{op}$, etc. are identical to those of $\widehat{\mathbf{E}}_0$, $\boldsymbol{\gamma}_0$, etc. and are given as equations (31).

We note that for a rod made of an isotropic material, equation $(A.4)_3$ becomes

$$2\mu A\boldsymbol{\gamma}_0 = \mathbf{T} + \mathbf{C}\mathbf{k},$$

where we have used $\boldsymbol{\gamma}_{op} = \mathbf{T}/2\mu A$ for an isotropic body. If $\mathbf{V}(\xi)$ in equation (21) is a skew-symmetric matrix, then the cross-section of the rod undergoes rigid rotations and hence is not deformed, and $\mathbf{s}$ in (A.1) could be an affine function of $\mathbf{r}$ and still satisfy $(24)_{14}$ and $(28)_2$.

References

1. R.D. Mindlin, *An Introduction to the Mathematical Theory of Vibrations of Elastic Plates*. U.S. Army Signal Corps Engineering Laboratories, Fort Monmouth, NJ (1955).
2. R.D. Mindlin, Forced thickness-shear and flexural vibrations of piezoelectric crystal plates. *J. Appl. Phys.* **23** (1952) 83–88.
3. E. Reissner, On the theory of elastic plates. *J. Math. Phys.* **23** (1944) 184–191.
4. P.G. Ciarlet and P. Destuynder, A justification of the 2-dimensional linear plate model. *J. de Mécanique* **18** (1979) 315–344.
5. W.T. Koiter and J.G. Simmonds, Foundations of shell theory. In: *Proc. IUTAM Congress*, Moscow (1972) pp. 150–176.
6. P.M. Naghdi, The theory of shells and plates. In: C. Truesdell (ed.), *Handbuch der Physik*, Vol. VIa/2. Springer, Berlin (1972).
7. S.S. Antman, The theory of rods. In: C. Truesdell (ed.), *Handbuch der Physik*, Vol. VIa/2. Springer, Berlin (1972).
8. A.W. Leissa, Recent research in plate vibrations, 1981-85, Part I: Classical theory; Part II: Complicating effects. *The Shock and Vibration Digest* **19**(2) (1987) 11–18; **19**(3) (1987) 10–24.
9. E. Cosserat and F. Cosserat, Sur la statique de la ligne deformable. *Compt. Rend.* **145** (1907) 1409–1412.
10. J.L. Ericksen, Plane infinitesimal waves in homogeneous elastic plates. *J. Elasticity* **3** (1973) 161–167.
11. P. Podio-Guidugli, An exact derivation of the thin plate equations. *J. Elasticity* **22** (1989) 121–133.
12. V. Nicotra and P. Podio-Guidugli, Piezoelectric plates with changing thickness. *J. Structural Control* **5** (1998).
13. L. Teresi and A. Tiero, On variational approaches to plate models. *Meccanica* **32** (1997) 143–156.
14. J.S. Yang and R.C. Batra, Mixed variational principles in nonlinear piezoelectricity. *Internat. J. Non-Linear Mech.* **30** (1995) 719–726.
15. S.S. Vel and R.C. Batra, Analytical solution for rectangular thick laminated plates subjected to arbitrary boundary conditions. *AIAA J.* **37** (1999) 1464–1473.
16. N.N. Rogacheva, *The Theory of Piezoelectric Shells and Plates*. CRC Press, Boca Raton, FL (1994).